Cycle-to-Cycle Control of Reconfigurable Die Sheet Metal Forming

by

Chester Dewey Vaughan IV

B.S., Mechanical Engineering
University of Alaska, Fairbanks, 2002

Submitted to the Department of Mechanical Engineering
in Partial Fulfillment of the Requirements for the Degree of
Master of Science in Mechanical Engineering

at the

Massachusetts Institute of Technology
[June Date]
May 7, 2004

Signature of Author .....
Department of Mechanical Engineering
May 7, 2001

Certified by .....
David E. Hardt
Professor of Mechanical Engineering
Thesis Supervisor

Accepted by .....
Ain A. Sonin
Chairman, Department Committee on Graduate Students

Cycle-to-Cycle Control of Reconfigurable Die Sheet Metal Forming

by

Chester Dewey Vaughan IV

Submitted to the Department of Mechanical Engineering
on May 7, 2004 in Partial Fulfillment of the
Requirements for the Degree of
Master of Science in Mechanical Engineering

ABSTRACT

This research addresses cycle to cycle control as applied to a sheet metal stretch forming process. More specifically, it attempts to validate the use of cycle to cycle (CtC) control for a multiple input-multiple output process. The work presented in this thesis attempts to answer some basic manufacturing questions. The first is, "Can a multivariable discrete system control theory be used to model a sheet metal shape control process?" The second question is, "Does such a "cycle to cycle control system provide a significant improvement over the present industry standard control methods". To address these questions, CtC control methods are applied to a reconfigurable die stretch forming process.

The theoretical foundation of the stretch forming process is presented. Several open and closed loop control methods are discussed. A methodology for evaluating the part quality is defined in terms of the process mean shift and variance. The system dynamics are presented in terms of unwanted process disturbances. In-depth experiments are then performed to quantify the process performance under CtC control. The CtC process yield is compared the process yield of an identical process under open loop control using the Expected Quality Loss Function.

It is shown that implementation of the reconfigurable die under CtC control eliminates the process mean shift but increases the part variation. It is also shown that CtC control produces the highest yield of acceptable parts.

Thesis Supervisor: David E. Hardt
Title: Professor of Mechanical Engineering

ACKNOWLEDGEMENTS

First, I want thank my Parents, Chet and Lynn Vaughan, for their love, support, and encouragement. I wouldn't be writing this if it weren't for them. I am also very grateful to my brother and sisters, Christine, Alex, Becky, Emily, and Kealy. Also, my Brother-in-Law Dusty, Nephew #1 Buddy, and Niece or Nephew #2 (on the way!!).

Thanks to Prof. Dave Hardt for being a great advisor. He also hosts the best Thanksgiving dinners complete with great food and a history lesson. Lisa dispensed reimbursements, Halloween fashion advice, and essential free-food alerts.

Adam and Bala were my Main Damies! Adam is one of the smartest people I have ever met. He was always made time to answer my questions (even the really ignorant ones). His help on my research project was invaluable. Bala made our lab the best MIT ever had. Somehow we managed to survive two years here and still remain mostly sane. We're sorry to all the people who were the butt-end of our practical jokes (not really). Sadatay!!

Thanks to Mark and Jerry for all the great machining advice. Leslie and Joan helped me get settled in and kept me on track. They always made sure I was properly fed and cared for. Carla, Larissa, and Xanat explored Boston with me. Jason led me on the best bike rides. Naomi helped me get through my first year of classes.

Finally, I owe so much to my girlfriend Johnna Powell. When I first came to MIT I thought I would be in-and-out in two years. I never thought I would meet someone so special that I would consider staying. I am constantly impressed and humbled by her accomplishments and will always be proud of her.

CONTENTS

FIGURES

CHAPTER

1

INTRODUCTION

1.1 Introduction

This research addresses aspects of cycle to cycle control as applied to a sheet metal stretch forming process. More specifically, it attempts to validate the use of cycle to cycle control for this application and benchmark several possible control methods.

1.2 Motivation for Study

This project stems from an industrial need for a reconfigurable sheet metal stretch forming machine. Stretch forming is used extensively in the airplane manufacturing process to form the sheet metal skins for the exterior of the airframe. Briefly, the current process consists of plastically stretched sheet metal being wrapped across the face of a shaped die. This will be discussed in much greater detail in subsequent chapters.

Unfortunately, because of elastic springback and lack of in-process measurement, etc..., the stretch forming process is very difficult to characterize analytically. The combined effects of these factors make it exceedingly difficult to accurately predict the proper die shape for any given part. The present solution to this problem requires a trial-and-error approach and excessive test runs to converge on the correct die shape. This procedure is expensive, time consuming, and relatively inaccurate.

1.3 Background

Traditional stretch forming is hindered by three fundamental problems; high capital costs, inability to effectively predict proper die shape, and excessive shape variation.

The tooling and machinery used in the stretch forming process is costly to produce and maintain. A typical airplane skin is composed of many different shapes ranging in size from wingtips to fuselage sections. Numerous dies need to be designed and produced to construct an airplane since each die can be used to produce only one shape. Notoriously low production volumes and large product variety mean that time and money consuming die changeovers are frequent. In addition, a lot of storage space is required to maintain the dies while they're not in service.

The design of conventional solid dies is more of an art then a science. It is typically an iterative process requiring several weeks and a great deal of machining time between iterations. The inability to analytically predict the proper die shapes results in many unacceptable parts while the dies are under development. This adds to the already high costs.

Non-standard operating procedures (SOP's) and control methods can also result in excessive shape variation. Stretch forming has many possible techniques for process control. These range from scientific methods such as monitoring pressure in the machine hydraulics or force or strain in the material, to low tech methods such as relying on the operator's visual estimate. Consistency in most all manufacturing processes is key to reducing variation. Work performed at MIT by Parris [1] and Valentin [2] concluded that implementing standard operating procedures and strain control can reduce process variation considerably. This is shown graphically in Figure 1.

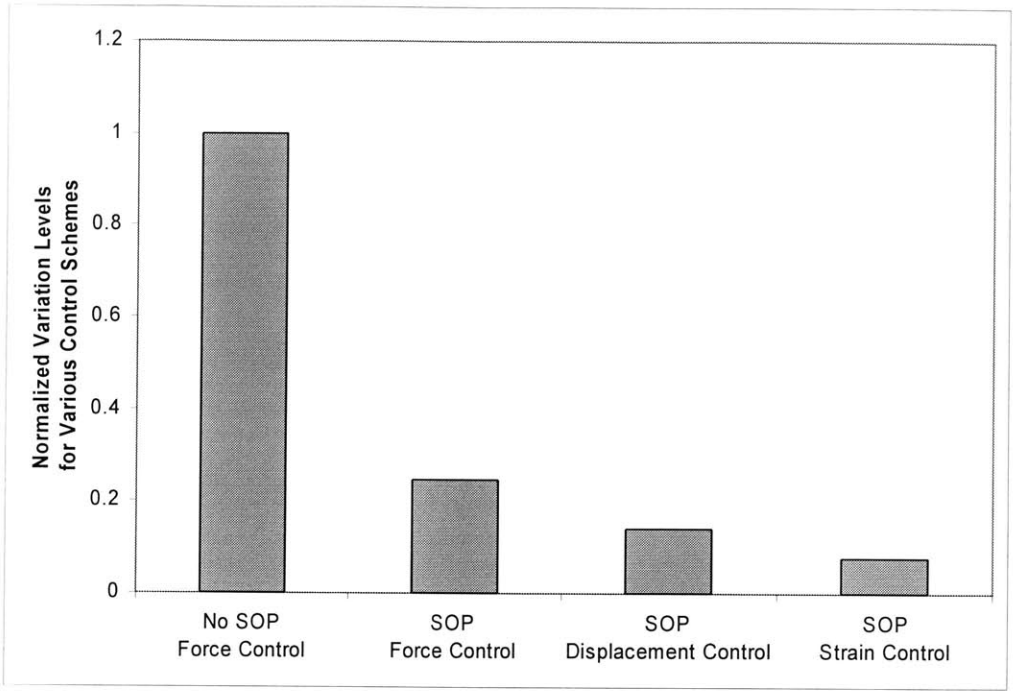

Figure 1: Variation levels associated with different process control strategies (SOP: Standard Operating Procedure), Diagram from Norfleet [8]

MIT, in cooperation with Northrop Grumman Corp. has developed a discrete die stretch forming machine. This machine was designed to circumvent many of the inadequacies inherent in the present day process by substituting a discrete bundle of pins in place of the conventional rigid die. The bundle is comprised of 552 discrete pins. These "forming pins" are ½" square pins located on ½" centers. The 552 pins are arranged in a rectangular bundle 24 pins high and 23 pins wide. The pins are rounded on the forming end. Each of these pins can be individually adjusted. This allows the die shape to be reconfigured in order to produce a wide range of part shapes.

1.4 Contributions of this Work

The work presented in this thesis attempts to answer some basic manufacturing questions. The first is, "Can a multivariable discrete system control theory be used to

model a shape control process?" The second question is, "Does such a "cycle to cycle control system provide a significant improvement over the present industry standard control methods". The following chapters will attempt to answer these questions by applying cycle to cycle control methods to a reconfigurable die stretch forming process. Chapter 2 will present the theoretical foundation of the stretch forming process. Several open and closed loop control methods will be presented in chapter 3. Chapter 4 explains the procedure for evaluating the part quality and discusses the system dynamics in terms of unwanted process disturbances. In-depth experiments are performed in chapter 5 to quantify the process performance under CtC control. The CtC process yield is compared the process yield of an identical process under open loop control using the Expected Quality Loss Function.

CHAPTER

2

OVERVIEW OF STRETCH FORMING

Stretch forming is a method by which a material's shape is altered by a specific combination of stretching and bending. The most common applications involve using a die to impart non-complex curves onto a sheet metal blank. The die is used to transfer a shape pattern to the blank (or part). Unfortunately, the part shape is rarely identical to the die shape that produced it. The die and part shapes match only when the part is in direct contact with the die. The part shape changes once the forming operation is complete as a result of residual elastic moments and stresses on the part experienced during the stretch forming process and is called springback. It is difficult to determine the springback of an arbitrarily shaped piece of sheet metal prior to forming. This leads to the difficulty in predicting a correct die shape to form a desired part shape. Stretch forming is an attempt to form a desired shape contour while minimizing springback. In order to understand the nature of springback, it is necessary to understand the physics of the stretch forming process.

2.1 Stretch Forming Theory

The stretch forming process is intended to significantly reduce the residual moments present in the workpiece following the forming operation. Stretch forming involves a stretching phase and a forming (or wrapping or bending) phase. The stretching phase can be implemented before forming, after forming, or both. Typically, a sheet metal part is formed by first stretching the workpiece along one direction. This changes the strain state of the material. The part is then formed by wrapping it across a shaped die. Once

the piece is bent across the die and released, the piece usually springs back as a result of residual moments within the piece. Stretching the workpiece beyond the yield stress, while the part is in contact with the die, minimizes the amount of springback that occurs after the forming process is complete.

Figure 2 illustrates the three phases of the stretch forming process. After the sheet metal blank has been loaded into the machine, an initial strain (ε_{Pre}), is applied to the material. The strain level can be increased or decreased by controlling the amount of force applied to the sheet. It is desirable to keep the strain state of the material constant during the forming phase. Different control modes, such as force, strain or displacement control can be used to govern the strain state. The orientation of the part during the forming phase can also be controlled in a variety of ways (e.g. jaw position, jaw motion, etc...).

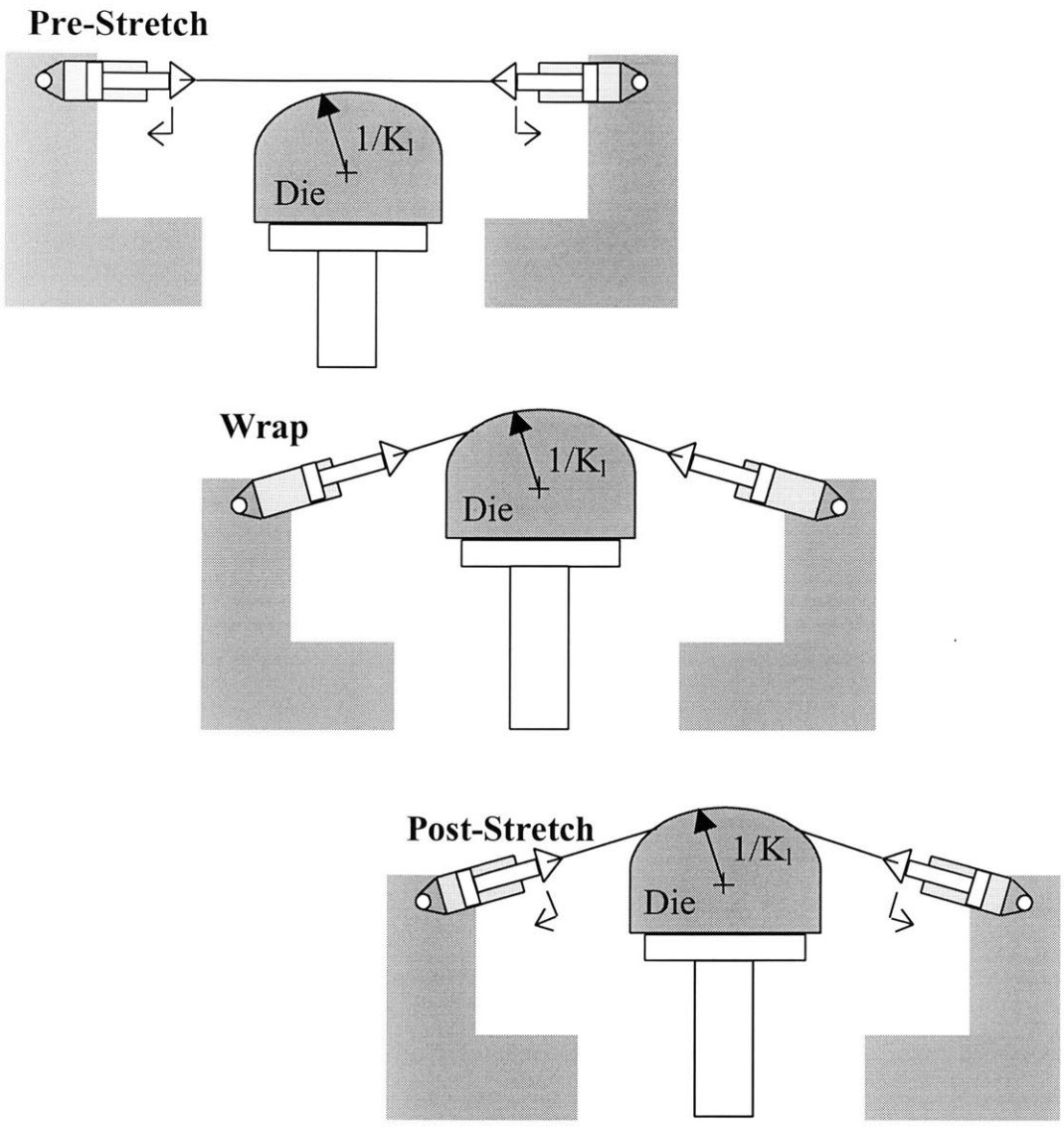

Figure 2: Illustration of stretch forming process on die of constant curvature (K_l)

Diagram from Norfleet [8]

The die is assumed to have a cylindrical curvature (K_l), where K_l is the inverse of the die radius ($1/R_l$) as can be seen in Figure 2. The following analysis is valid for shapes of constant curvatures.

During the pre-stretch phase, the sheet is clamped at the ends and stretched uniformly across the width of the piece until the desired strain state is reached. The strain

state throughout the material thickness, (ε(y)) is defined through any cross section by Equation 1:

$$\varepsilon(y) = \varepsilon_{pre}$$

Equation 1

Where:

ε= *strain state*

y= *position from neutral axis*

ε_{pre} = *pre-stretch strain value*

The resulting stress and strain states are shown in Figure 3. During the pre-stretch phase, both the stress and strain are uniform across the width of the workpiece.

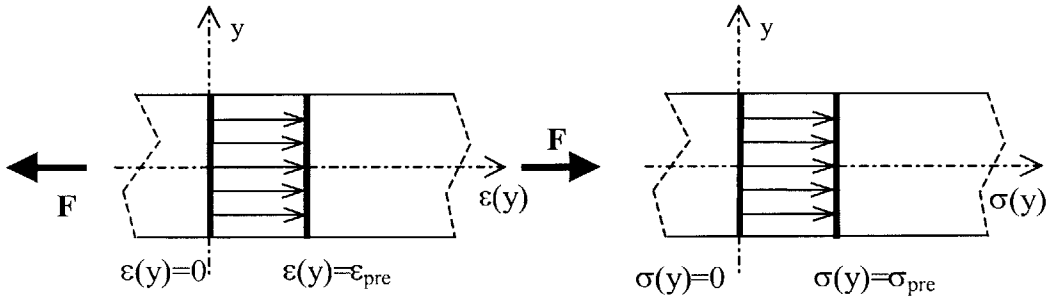

Figure 3: Stress and strain distribution in workpiece during pre-stretch phase

Diagram from Hardt [3]

The material is assumed to be elastic-perfectly plastic in order to simplify the analysis. Equation 2 and Equation 3 describe the stress state for an elastic-perfectly plastic material. This approximation is sufficient for materials commonly used in the stretch forming process.

$$\sigma = E\varepsilon \quad \varepsilon < \varepsilon_{yield}$$

Equation 2

$$\sigma = \sigma_{yield} \quad \varepsilon \geq \varepsilon_{yield}$$

Equation 3

Where:

σ = *stress state*

ε = *strain state*

ε_{yield} = *strain value at yield stress*

σ_{yield} = *yield stress value*

E = *Young's Modulus*

During the forming phase, the workpiece is bent across the die. The workpiece is assumed to be under simple bending for the purposes of this analysis. The stress and strain distributions for simple bending (no pre-stretch) are shown in Figure 3 and Figure 4.

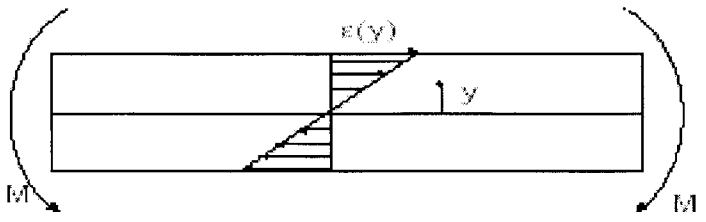

Figure 4: Strain distribution of material in simple bending

Diagram from Hardt [3]

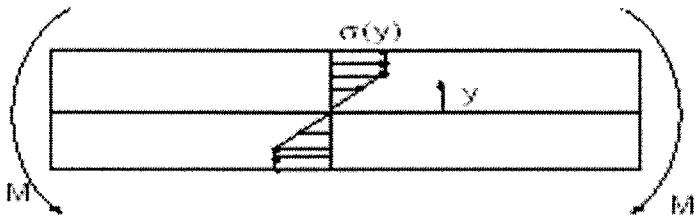

Figure 5: Stress distribution for elastic-perfectly plastic material in simple bending.

Note that the outer fibers have stress values that are in yield as a result of elastic-perfectly plastic behavior and high strain levels. Diagram from Hardt [3]

In stretch forming, the total strain experienced by the workpiece during the forming phase is the sum of the strain contributions from the pre-stretch and bending phases. This can be observed graphically by adding Figure 3 to Figure 4 and Figure 5. This will result in Figure 6 and Figure 7.

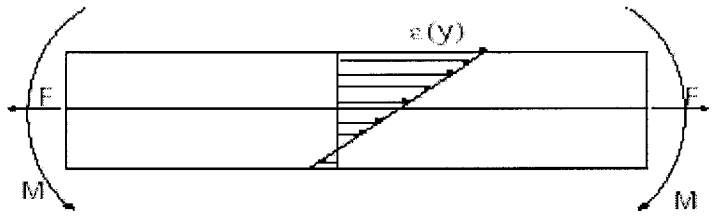

Figure 6: Total strain distribution in workpiece during wrap phase

Diagram from Hardt [3]

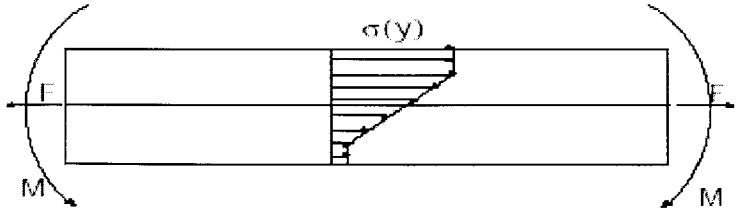

Figure 7: Total stress distribution in workpiece during wrap phase

Diagram from Hardt [3]

An elastic-perfectly plastic material will exhibit a perfectly uniform stress state (across the width of the workpiece) if the lowest value of strain in the workpiece is above the yield strain. With sufficient pre-stretch strain, Figure 6 will appear as Figure 8, where all strain values in the workpiece are above the yield strain value.

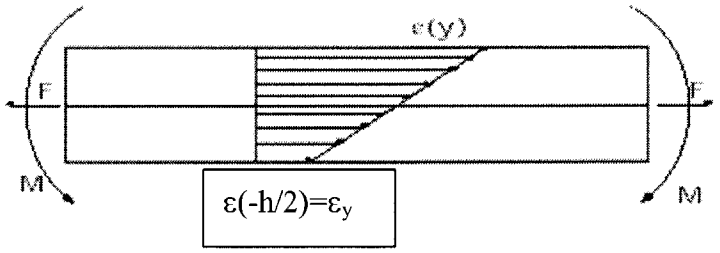

Figure 8: Strain distribution with all strain values above yield

Diagram from Hardt [3]

As mentioned previously, the stress states for an elastic-perfectly plastic material will be uniform if all strain values across the workpiece are above yield. An elastic-perfectly plastic material with a strain distribution as shown in Figure 8 will have a uniform stress distribution as shown in Figure 9.

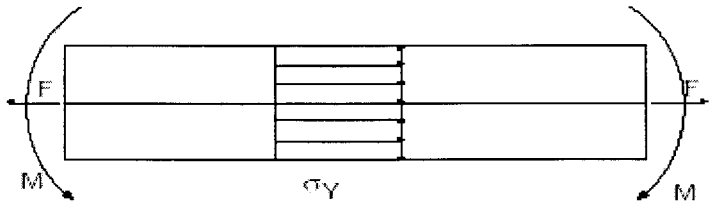

Figure 9: Stress distribution in workpiece with all strain values above yield

Diagram from Hardt [3]

It should be noted that post-stretching, in lieu or in tandem with pre-stretching, will satisfy the theoretical requirements as well. All that matters is that the strain values across the workpiece are above yield while the die is in contact with the workpiece.

A uniform stress distribution across the workpiece (during forming) will result in no curvature springback in the workpiece after forming is complete. This is due to the lack of any residual moments in the workpiece. The rationale for this is detailed in Equation 4.

$$M_l = \int_{-h/2}^{h/2} \sigma(y) y w dy$$

Equation 4

Where:

M_l = *moment in workpiece*

w = *workpiece thickness*

h = *workpiece width*

$\sigma(y)$ = *stress distribution in workpiece*

M_l represents the moment in the workpiece. For a uniform stress distribution, M_l will become zero. As a result, if a sufficiently large pre-stretch strain is applied, there will be no residual moment, and no springback in the workpiece.

Most materials are not elastic perfectly-plastic. Fortunately, many useful materials, such as 2024-O aluminum, are similar enough to elastic-perfectly plastic materials that we can utilize the stretch forming theory. Although the final stress distribution during stretch forming will not be exactly uniform for materials such as 2024-O aluminum, the stress distribution will be close to uniform, and will significantly reduce the springback of the workpiece. However, if no pre-stretch (or post-stretch) strain is applied, and/or the material is not close to the elastic-perfectly plastic model, then a greater amount of

springback will occur. This problem is readily apparent for parts of very low curvature because the material may achieve the proper curvature without passing out of the elastic range. The workpiece will spring back to the initial shape once the bending load is removed since the forming operation never caused the material to be strained beyond yield. The results from this analysis illustrate the benefit of stretch forming, as opposed to merely bending a workpiece without any pre-stretch.

2.1.1 Springback Quantification

The term "springback" refers to the net shape change that occurs after relaxation of the stretch forces. For a simple curve, it is the shape difference between the curvature of the loaded workpiece (K_l) and the curvature of the unloaded workpiece (K_u). The springback ratio (ΔK) describes the relationship between the loaded and unloaded curvatures of the workpiece. The springback ratio for shapes of constant curvature (i.e. cylinders) can be analytically described by Equation 5.

$$\Delta K = \frac{K_l - K_u}{K_u}$$

Equation 5

Where:

ΔK = *springback ratio*

K_l = *curvature of workpiece when loaded*

K_u = *curvature of workpiece when released*

Although most stretch formed shapes are not simple cylinders, this shape is useful to illustrate the effects of springback during the stretch forming process.

Springback analyses for non-constant curvature parts have also been developed for some parts. Parris [1] developed one such analysis for springback. However, the

application of such an equation was limited to two-dimensional shapes where the curvature of interest lies along one plane. Springback analyses for three-dimensional parts are more complex and difficult to perform.

2.2 Industrial Application

Stretch forming sees widespread use in most industries that require sheet metal parts of slight curvature. These are primarily the aerospace (aircraft) and marine industries (boats, submarines. These industries produce assemblies (e.g. planes, boats, submarines, etc...) of which significant portion of the components are comprised of curved sheet metal skins. Conventional stretch forming is a capital and time intensive process. The stretch forming process is heavily dependent on operator expertise, and delays are prevalent because of a trial and error approach. High levels of part error are common.

2.2.1 High Capital Costs

In the aerospace industry, stretch forming is traditionally performed using solid dies such as the one shown in Figure 10. The die is typically composed of a soft metal, polymer, or polymer composite. The use of monolithic dies in the stretch forming process has several benefits. The die is very stiff and durable and with proper maintenance will usually have a very long production cycle. Monolithic dies produce very little part variation since the dies are usually extremely rigid. They are also simple to use once installed in the press.

Unfortunately, they suffer from many drawbacks as well. Proper manufacture of monolithic dies requires specific expertise and machining capabilities. This is typically neither cheap nor readily available. Monolithic dies are usually machined from a solid block of material using various manufacturing processes. Larger dies are more difficult to manufacture, use, and store. Dies commonly used in the stretch forming process can weigh between 1,000 and 20,000 lbs. and cost from $10,000 to well over $100,000 [6].

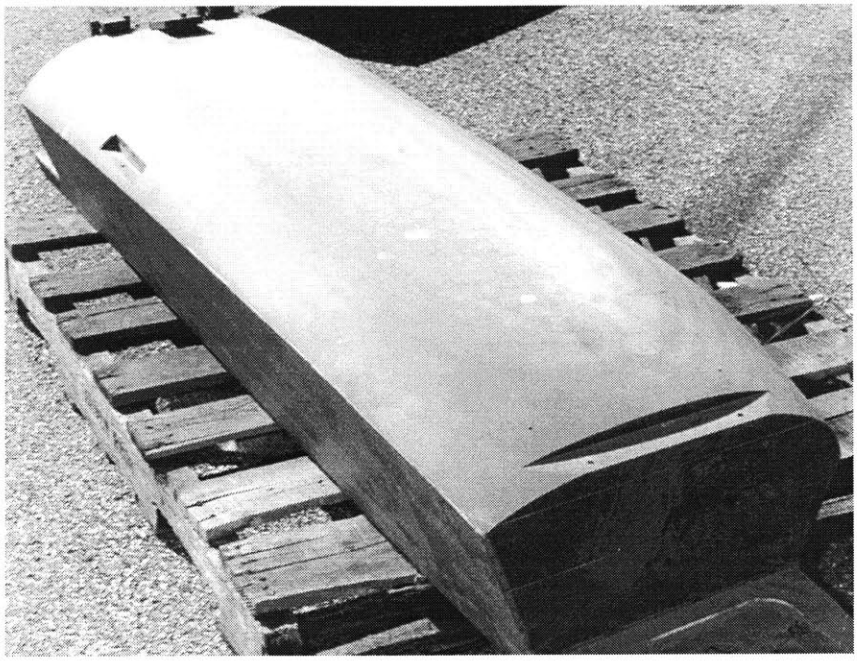

Figure 10: Solid die used in manufacturing leading edge airplane parts

(Photograph Courtesy of Northrop Grumman)

Making a die, such as the one shown in Figure 10, can take several weeks. This will usually be followed by several more weeks of adjustment or fine tuning which could easily cost several thousand dollars. The die in Figure 10 is approximately 2 x 6 x 1 feet. These dies can range from small wing tip sizes to a large Boeing 747 fuselage section. Each airplane is composed of many different stretch formed parts. Hundreds of dies can be necessary to form parts for a single aircraft. Each of these dies has an associated manufacturing, inventory, and maintenance cost.

Time is money in a manufacturing environment. The initial tool manufacturing lead time averages 12 weeks [4]. This represents the time from when the engineering drawing is received to when the first part is formed. The part accuracy (reflected in the process centering) is a function of how accurately the die shape is suited to the desired part shape. Stretch forming dies are difficult to design since so many factors other then die shape (i.e. material, stretch force, machine states, etc…) affect the final part shape. The proper die shape largely depends on the size, material, and shape of the part being formed and is very difficult to accurately predict. Therefore, additional time must be spent reworking

the die shape to improve part accuracy. This usually takes place after the die is delivered to the production line and typically takes at least as long as tool design and fabrication combined.

Size, complexity, tool material, and application all contribute to the final tool cost. The cost of tooling is eventually passed on to the consumer in the form of an increase in the purchase price. The price increase on a per part basis will depend on the size of the production run. The burden of tooling cost can be very prohibitive for job shops or other manufacturing operations with small production runs.

Stretch formed parts in the aerospace industry are typically formed in small batch or lot sizes. A lot size of one part is not uncommon for a repair facility. Tool, or die, changeovers are common as a result of this. Although improvements have reduced the changeover time of dies to approximately an hour, this is still significant time and money devoted to a non-value adding process. This does not account for costs associated with retrieving or tracking a die as well.

To address this issue, research at MIT over the past two decades has been aimed at developing a reconfigurable tool. The laboratory scale die is approximately 1ft x 1ft in area, and is composed of 552 discrete pins. The tool, designed by Robinson [5] and refitted by Valjavec, [6] is shown in Figure 11. Northrop Grumman, in a joint project with MIT and Cyril Bath Inc., designed and manufactured a production scale tool of approximately 35ft x 6ft with over 2000 pins [7]. This tool is shown in Figure 12. The purpose of creating a reconfigurable tool was to reduce the changeover times and costs associated with the traditional stretch forming process by constructing a die with a reconfigurable forming surface. Both reconfigurable tools are composed of discrete, spherical tipped, square pins. These pins can be moved independently, altering the part shape as desired.

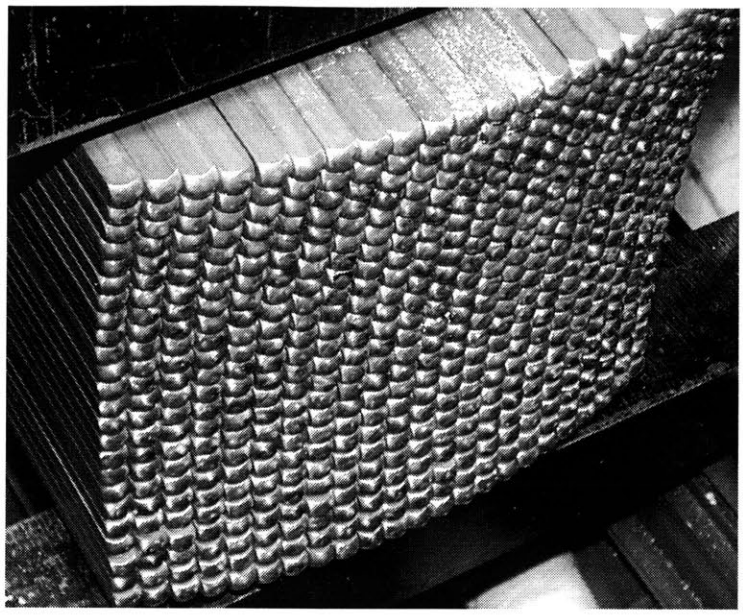

Figure 11: MIT reconfigurable die

Composed of 552 pins (24 x 23). Each square pin is 1/2" in width. The die elevations are positioned with 8 servos.

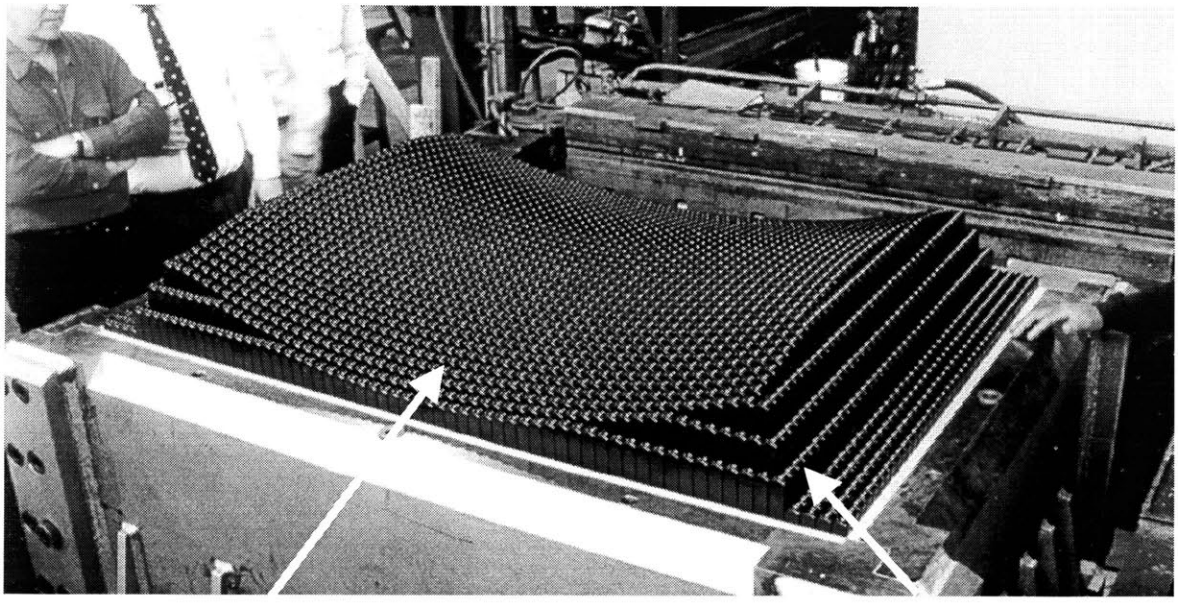

Figure 12: Northrop Grumman reconfigurable die

Made up of 2688 discrete pins of 1 1/8" width and positioned by 2688 servos. Photo from Papazian [9]

Although there are differences between the MIT and Northrop Grumman tools, the overall functionality is similar. The size of each of the discrete pins determines the minimum curvature that can be formed by the tool. Smaller pin sizes allow larger part curvatures. Stretch formed parts in the aerospace industry typically have slight curvatures. Northrop Grumman determined that a pin size of 1 1/8" would suffice for a large fraction of aircraft parts. The tool MIT developed uses ½" pins.

Monolithic dies are manufactured with a smooth forming surface. This, in turn, forms a smooth part surface since the part is exposed to a smooth contact pressure. Discrete dies simulate the smooth surface only at the pin tips. A flexible, intermediate surface must be used to bridge the gaps between the pin tips and even out the contact pressure seen by the part (see Figure 13). This avoids the "dimpling" effects of the discrete pins on the sheet metal. This intermediate surface is called the interpolator and is usually a rubber or plastic of some sort, (typically Ethylene Vinyl Acetate, Polyurethane, Elvax, or some other material with favorable compliant material properties). The surface of the interpolator is typically treated in some manner to reduce the frictional effects between the sheet metal and interpolator. Coating the interpolator with a lubricant, or using a thin Teflon sheet(s) are among the preferred methods. In general the thickness of the interpolator is determined by the thickness of the pins. It has been found that for optimal performance, the thickness of the interpolator and pin width should be approximately equal [7].

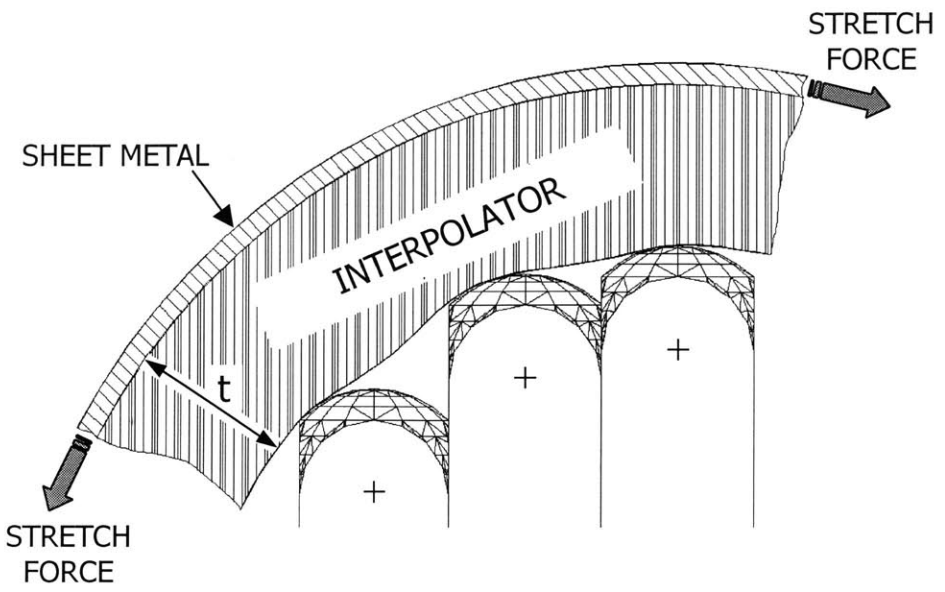

Figure 13: Illustration of interpolator

Pin and interpolator thicknesses are approximately equal. There is a smooth contact surface for the sheet metal workpiece, which results in no dimpling. Diagram from Norfleet [8]

One of the greatest benefits of using a reconfigurable tool is the reduction in changeover times. Added benefits also include an overall reduction in the number of dies as well as a reduction in the costs associated with maintaining those dies.

The reconfigurable tool lends itself remarkably well to "emergency" or "priority" orders. In the aerospace industry, a significant portion of part orders for stretch formed parts goes towards repairing grounded planes [9]. The parts required are highly variable and will be in extremely small batch and lot sizes (often only one unit of a particular part will be required). However, even with the reconfigurable tool, some means of determining the correct die shape for a desired part shape is required.

As discussed in the previously, die prediction is difficult because of the springback effect. The preceding analysis was limited to constant shape curvatures. In industry, die shapes of a constant curvature are a rarity. This problem is further compounded by the discrete die since the forming surface is actually made up of hundreds or thousands of

complex curves. The addition of the interpolator prevents dimpling, but is another unknown in an already difficult problem. The properties and physics of the interpolator are not exactly known and cannot be sufficiently predicted. Although the reconfigurable tool reduces the changeover time necessary in stretch forming, it makes shape prediction more difficult. Effective shape control is even more important with the reconfigurable tool as a result of these additional issues.

2.2.2 Shape prediction Issues

As previously discussed, springback is difficult to predict for all but the simplest cases. Variations in material properties and uncertainty about the interpolator behavior limit the accuracy and usefulness of analytical methods in precisely estimating springback. In lieu of analytical methods, die designers have traditionally used experience and guesswork to chiefly determine the proper die shape. The current die development process is typified by a time-consuming die rework procedure as shown in Figure 14.

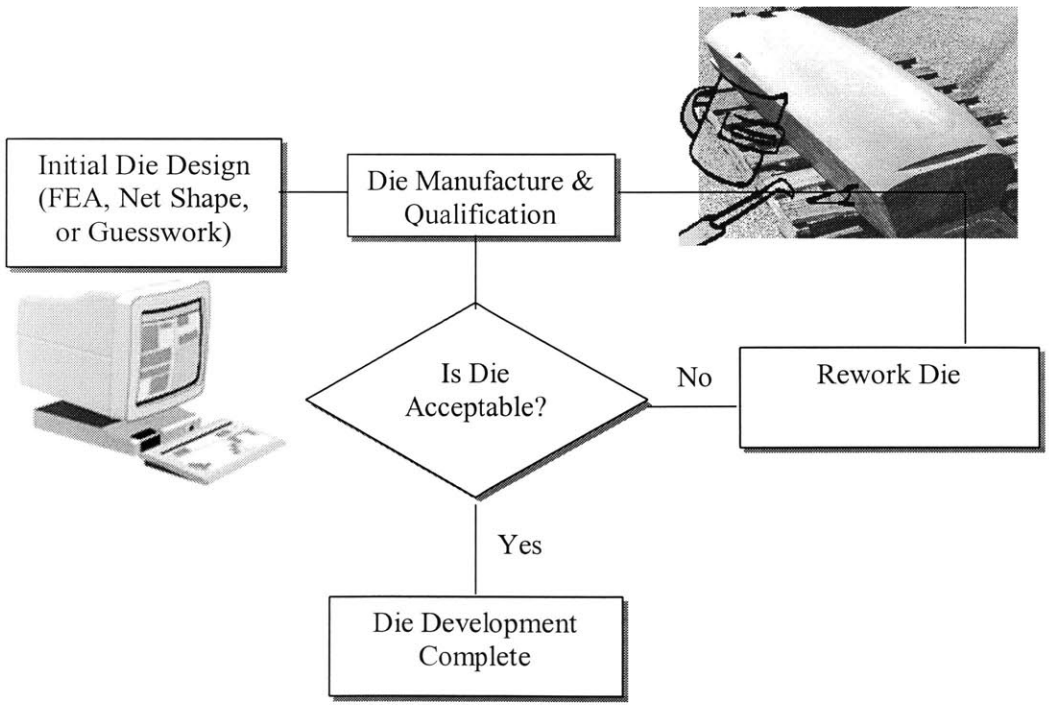

Figure 14: Iterative die manufacturing procedure

Diagram from Norfleet [8]

As observed in Figure 14, finite element analysis (FEA) may be used to create an initial die guess. However, after this first guess, a trial and error approach, based on operator expertise, is commonly used for successive iterations. Increased part variation and decreased part quality often results from this unintentional input of human error. This iterative cycle could take weeks if a monolithic tool required modification. A reconfigurable tool would reduce this rework period to days. Valjavec [6], Norfleet [8], and Pi [10] cover FEA simulation of stretch forming dies in greater detail.

2.3 Summary

This chapter covered the basic concepts of stretch forming. The physics of the stretch forming process were discussed, and the causes of springback were examined. The status quo stretch forming process is hindered by two major fallacies. The first is the costs associated with manufacturing and maintaining a large number of different dies. The second is the iterative methodology used in die shape prediction. These issues have been partially addressed through a reconfigurable tool jointly developed by MIT and Northrop Grumman.

CHAPTER

3

PROCESS CONTROL METHODS

This chapter reviews work previously published by Valjavec [6], Siu [17], Norfleet [8], Pi [10], Rzepniewski [16], and Hardt[3]. The following sections examine manufacturing process control methods as applied to the reconfigurable die stretch forming process. The basis of cycle to cycle control is established and several control algorithms are presented.

3.1 Manufacturing control methods

All manufacturing processes are controlled to some extent. Manufacturing controls are used to govern the outputs of a system. There is a hierarchy of system outputs. We are chiefly concerned with the primary outputs. In our case, the primary outputs are the part shape, material thickness and dimensions, etc... These primary outputs are directly affected by secondary outputs such as stretch force, die shape, die orientation, and hydraulic pressure among many others. The goal of process control is to deliver an acceptable primary output. Satisfying this goal may require controlling any number of primary and/or secondary outputs.

Process controls can range from passive process monitoring to highly sophisticated, high bandwidth machine and process control systems. The level of control is usually dependent on the acceptable tolerances of the process output. Stricter tolerances will require tighter controls to satisfy them. There are two broad types of control. These are open loop control and closed loop control.

3.1.1 Open Loop Control

Open loop control is the simplest control method. Open loop control is characterized by Figure 15.

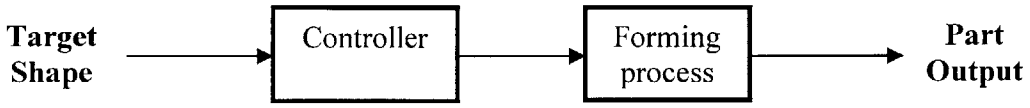

Figure 15: Open loop control diagram

We can see from the diagram that there is no means for information to flow upstream. Therefore, any data obtained through measurement cannot be used to adjust the processes upstream. This method utilizes a "set it and forget it" approach (find a combination of machine and/or process settings that produces a satisfactory primary result and not deviate from it).

The next level of control is Statistical Process Control (SPC). This method was pioneered by Tagutchi and others [11] and involves using the primary outputs to identify sources of systematic variation. Systematic variations, or assignable causes, are those variations which have a clear, or "assignable", source and may be eliminated [12]. The process is considered to be at its minimum variation state once these sources are identified and removed from the system. This state is termed "in control". SPC is characterized by run charts, Xbar charts, and S charts. These charts are used to verify that the process has not become subject to any assignable causes and remains "in control". SPC is very much an open loop control method since it is merely a process monitoring tool. It does not propose any corrective actions, let alone implement any process adjustments. It is left to the operator to determine and correct the cause of the variation once an out of control state has been signaled.

3.1.2 Closed Loop Control

Closed loop, or feedback, control involves an *a priori*, explicit process model and uses process data to alter the inputs and achieve the desired output. This control method allows information about the states of the process to flow upstream. There are three levels of feedback control. These levels can be combined to optimize system performance. Each of these levels follows a distinct information loop. All loops pass through the process controller first. The difference between the levels resides in the type of information that is transferred back upstream. This is depicted in Figure 16.

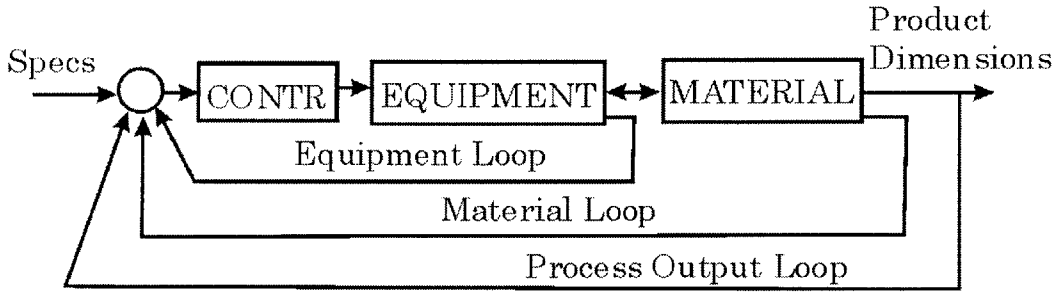

Figure 16: Process information feedback loops

Diagram from Rzepniewski [18]

The first level of closed loop control involves the equipment loop. This level is most common since it is the easiest to implement. Here, information about the equipment states is transferred back to the process controller. The controller directs the machine to generate a predetermined set of poses that should result in acceptable primary outputs. Although the machine is aware of its own states, it has no knowledge of the material states and properties. Therefore, it cannot adjust its own states to compensate for variation in the material states and properties (e.g. material stiffness, temperature, etc...).

The second level of closed loop control feeds back information regarding the material state. This control method has the ability to compensate for material variation. In a fashion similar to equipment loop feedback, the controller uses this data to infer process input adjustments that will result in acceptable primary outputs. Material stress,

strain, and temperature are potential candidates for material loop feedback. This type of feedback is rarely used due to the difficulty and expense associated with obtaining and responding to data.

The third level of closed loop control feeds back information about the process output. This method is distinguished from the previous methods by the direct feedback of the states and properties of the primary outputs. This means that the process controller can act on actual data regarding the primary outputs instead of having to infer what the outputs will be.

Closed loop control processes can be sampled and fed back at a variety of intervals. In-process control involves feeding back the appropriate process data at a frequency greater then once per cycle. This allows for changes to the process while the operation is still occurring. This is the preferred situation to apply closed loop control. However, in some processes, the appropriate output data cannot be fed back while in-process. Stretch forming is one of these processes. It is extremely difficult to measure the part shape in-process. In addition, springback will cause unpredictable part deformation once the process is completed and render the part shape measurement inaccurate. This limits the sampling frequency to a maximum of once per forming cycle. Closed loop control performed at the cycle frequency is termed Cycle to Cycle control (CtC). Rzepniewski, Hardt, and others cover this subject in greater detail [18].

3.1.3 Characteristics of CtC Control

As previously discussed, cycle to cycle shape control can be expressed as a discrete control block diagram. The block diagram shown in Figure 17 is the basic CtC control loop used in the stretch forming process.

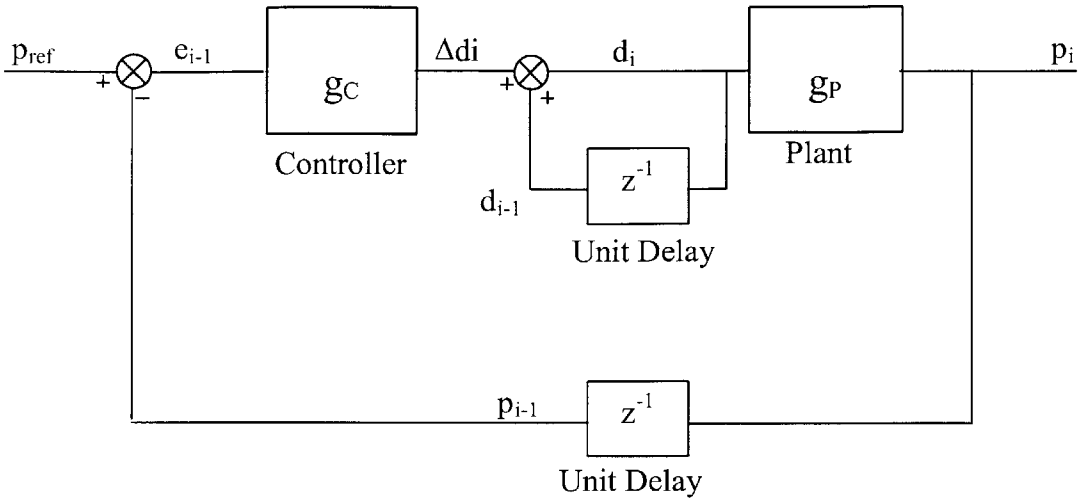

Figure 17: Block diagram model of the stretch forming process

g_c is the controller gain, determined by the user, g_p is the plant or process gain, which represents the behavior of the process. P_{ref} is the reference input and P_i is the part output. Diagram from Pi [10]

The process begins with an initial 'best guess' die shape (d_i). This die is used to create the first part (p_i). The stretch forming process is represented by gain factors associated with the process model, or plant (g_P). The first cycle of the process is completed with the forming of the first part. The index is thus changed from *(i=1) to (i=2)* making the first part (p_{i-1}). This is represented in the schematic by the z-transform unit delay (z^{-1}). The part shape error (e_{i-1}) is then calculated for (p_{i-1}), and multiplied by the controller gain factors (g_C). The controller uses the error and its gain factors to define what changes should be made to the die (Δd_i). These changes are then added to the previous die shape (d_{i-1}) to form the next die shape (d_i). The additional unit delay in this portion of the schematic represents the system's memory of the previous die shape. A new part is formed and the cycle continues. The process controller will gradually converge upon the proper die shape that will produce an acceptable part. The speed of convergence depends on the system response time.

3.1.4 Stretch Forming Shape Control

The shape control model has been developed over the past 23 years. Although the algorithm has been refined and applied to different processes by Webb [13,14], Osterhout [15], and Valjavec [6], the underlying structure of the control algorithm has not changed. In all cases the goal has been to converge upon a die shape that will yield the desired part shape (based on measurements of the prior part shape).

3.1.5 Controller Gains

As mentioned previously, the process begins with a "best guess" initial die shape. This "best guess" is typically the result of FEA analysis, prior historical results, or simply operator intuition. The initial die is used to form the first part. Upon completion of the first cycle, the shape of the first part is measured and compared to the desired (reference) part shape. If the first guess is an acceptable shape, there is no further need to continue.

It is most likely that the first part will not be within acceptable limits. This will trigger a die shape adjustment. The magnitude of the adjustment will be in proportion to the magnitude of the shape error. This proportional gain, or controller gain, is set to a value that yields desirable system performance. The next part is formed using a new die estimate based on the algorithm used. The new part is then formed and the errors compared again. The algorithm is continually repeated until an acceptable part is made. The generic algorithm can be expressed as an equation and is shown in Equation 6. This can be expressed in the equivalent matrix form shown in Equation 7:

$$\underline{d}_i = \underline{d}_{i-1} + G_C(\underline{p}_{ref} - \underline{p}_{i-1})$$

Equation 6

$$\underset{(MN,1)}{\begin{bmatrix} {}_1d_i \\ {}_2d_i \\ \vdots \\ {}_{MN}d_i \end{bmatrix}} = \underset{(MN,1)}{\begin{bmatrix} {}_1d_{i-1} \\ {}_2d_{i-1} \\ \vdots \\ {}_{MN}d_{i-1} \end{bmatrix}} + \underset{(MN,MN)}{\begin{bmatrix} {}_{1,1}g_C & {}_{1,2}g_C & \cdots & {}_{1,MN}g_C \\ {}_{2,1}g_C & {}_{2,2}g_C & \cdots & \vdots \\ \vdots & \vdots & \ddots & \vdots \\ {}_{MN,1}g_C & \cdots & \cdots & {}_{MN,MN}g_C \end{bmatrix}} x \left(\underset{(MN,1)}{\begin{bmatrix} {}_1p_{ref} \\ {}_2p_{ref} \\ \vdots \\ {}_{MN}p_{ref} \end{bmatrix}} - \underset{(MN,1)}{\begin{bmatrix} {}_1p_{i-1} \\ {}_2p_{i-1} \\ \vdots \\ {}_{MN}p_{i-1} \end{bmatrix}} \right)$$

Equation 7

Where:

d_i= *vector representing die shape for the* i^{th} *cycle in Cartesian coordinates*

p_i= *vector representing part shape for the* i^{th} *cycle in Cartesian coordinates*

p_{ref}= *vector representing reference part shape*

G_C= *matrix of controller gains*

The controller gains (G_C) are therefore a matrix of (MN) x (MN) dimension. This is because a gain value is needed to relate every location on the part to every location on the die. The matrix form of the algorithm is useful because the controller matrix can illustrate the relative influence among the different die and part locations. The diagonal of this gain matrix corresponds to the effect that each point on the die had on the corresponding part location. The off-diagonal terms are a measure of the degree of "coupling" between adjacent die and part locations. Coupling describes the influence an individual die location will have on the shape of adjacent part locations.

The dimensions of the matrix (MN x MN) changes several times throughout the cycle (the proportion remains the same however). For example, the die is considered to be a grid of M by N pins where M=10, N=11 in the region of interest, also known as the active region. Only the active region is measured and considered during the forming process. On the lab scale tool at MIT, this corresponds to an active region area of approximately 4.5"x 5". However, it is sometimes desirable to view the parts and dies with finer spacing than those of the die pins in the actual active region. When measuring and representing the die and part for system identification, a grid of M=46, N=51 points

is used. This is much finer than the physical die, but the points that correspond to the physical die can be determined using common interpolation techniques.

3.1.6 Process Gains

The plant matrix or process gain (shown as G_P in Figure 17: Block diagram model of the stretch forming process) is estimated using Equation 8.

$$G_P = \frac{P_2 - P_1}{D_2 - D_1}$$

Equation 8

Where:

P_1= *First part formed*

P_2=*Second part formed*

D_1=*First die used*

D_2=*Second die used*

As shown, the process gain is experimentally generated based on the first two forming cycles. This step could potentially be bypassed if the process gains had been previously determined during a prior run of similar parts. Unfortunately, system disturbances produce process mean shifts that might force a recalculation of the plant matrix. This is discussed in greater detail in section 4.5. Similar to the controller gain matrix, the plant matrix will have dimensions (MN x MN). The diagonal terms that illustrate the influence that each pin has on the corresponding part location. The off-diagonal terms will be a measure of the degree of coupling between different die and part locations.

3.1.7 System Response Time

Forming cycles that do not produce a part of acceptable quality are an expense in a manufacturing environment. Minimizing the number of iterations needed to form a desired part is of paramount importance when developing a control algorithm. The root locus method is a useful tool for analyzing the closed loop system response time. This analysis requires the open loop transfer function of the system which can be derived from the block diagram shown in Figure 17. The open-loop transfer function for the process is defined by Equation 9.

$$\frac{p_i}{p_{ref}} = \frac{g_C g_P z}{z(z-1)}$$

Equation 9

Using the root locus techniques we determine that the open loop transfer function has two poles and one zero. The zero is on the real axis and the poles are located at 0 and 1 as shown in Figure 18. The pole at 0 is "cancelled" by the zero on the real axis. This effectively leaves one pole located at 1 on the real axis. Therefore, the root locus for all closed loop gain values is a line extending from positive 1 to negative infinity as shown in Figure 18.

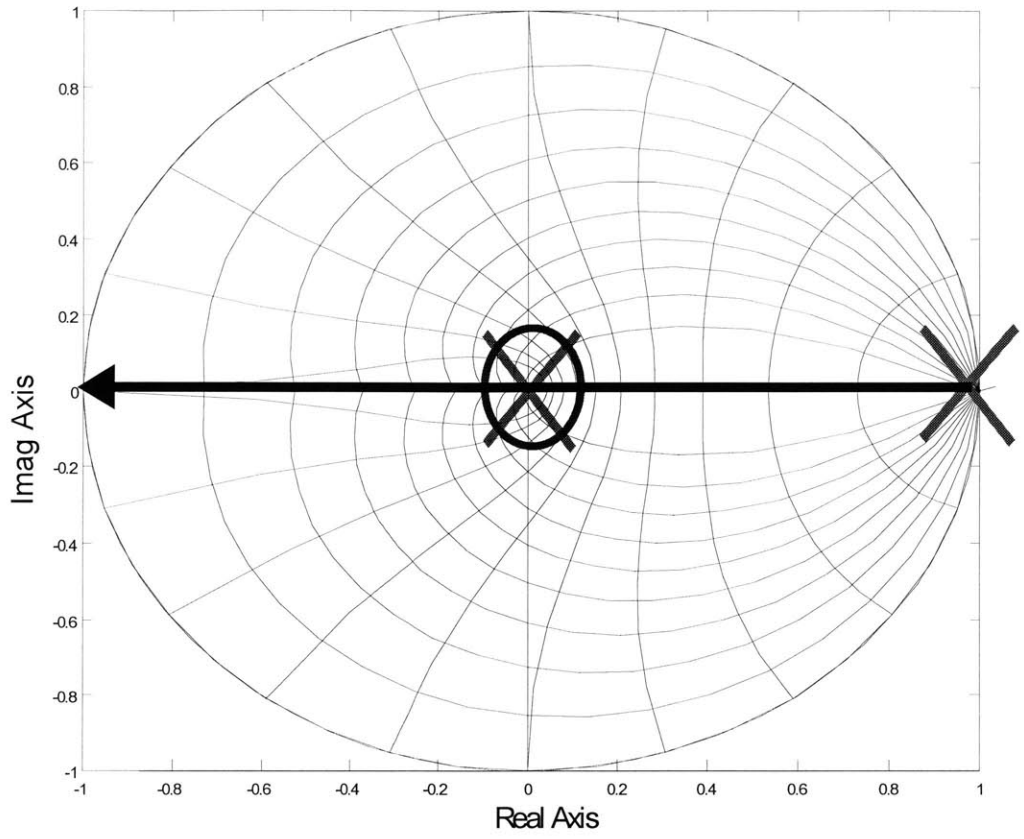

Figure 18: Root Locus for stretch forming closed loop CtC control in the z plane

Diagram from Norfleet [8]

It is assumed that g_C and g_P are constant gain values and are the same for each cycle where the closed loop shape algorithm is applied. The results of the root locus analysis allow us to predict the system response based on the loop gain (K) defined by Equation 10.

$$K = g_C g_P$$

Equation 10

For loop gains K, such that 0<K<1, the process response will be similar to that of an overdamped system. As the value of K approaches 1, the system response will be quicker, requiring fewer cycles, or time steps to reach the steady state value. Loop gain values K<1 result in overdamped system behavior while loop gain values of 1<K>2 result in oscillatory behavior. Loop gain values K>2 will cause the system to become unstable. A loop gain value of 1 is ideal as this will cause the system to settle in one cycle.

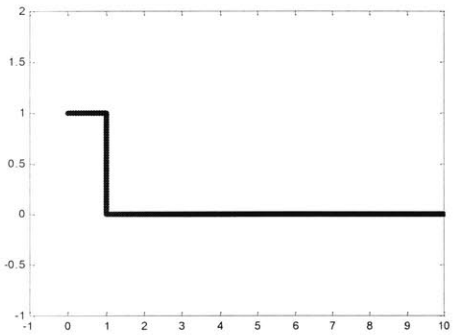

Input (Impulse)

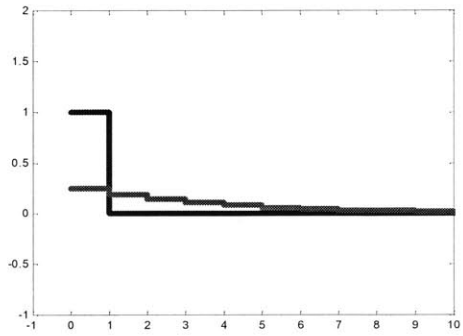

Output (GcGp=0.25)

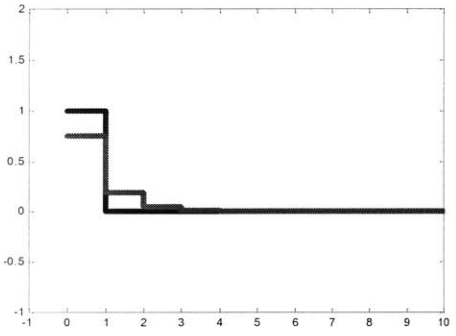

Output (GcGp=0.75)

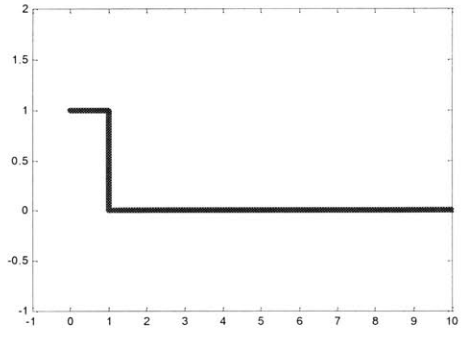

Output (GcGp=1)

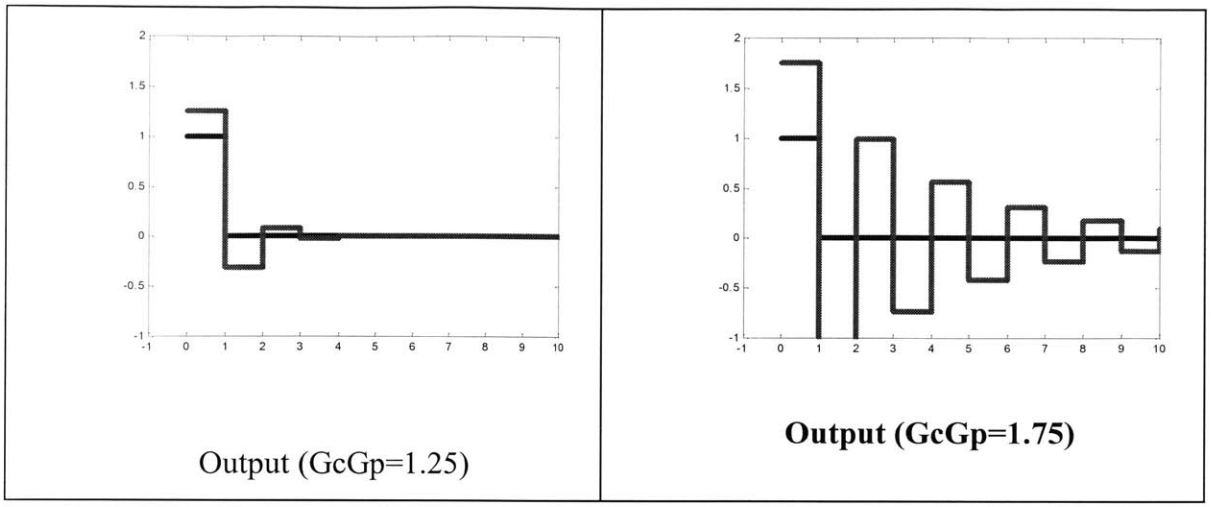

Figure 19: Graphs of system step responses at different loop gain values

Diagram from Norfleet [8]

Figure 19 illustrates the system response to different loop gain operating conditions. The condition where the loop gain K=1 is referred to as a "deadbeat" controller. It can be observed that the control algorithm will converge upon the proper die shape quickest if the overall loop gain is unity. The control algorithms used in these experiments define the controller gain (g_c) such that the overall loop gain K=1.

The analysis done here is only valid for a single input, single output system (SISO). For stretch forming with a discrete die, each pin and part location can be regarded as an input and output, resulting in a multiple input, multiple output system (MIMO). Rzepniewski and Hardt [16] extend the SISO analysis in this chapter to MIMO systems.

3.1.8 Steady State Error

The goal of closed loop control is to form parts that are identical to the reference part. The shape control algorithms have been designed such that their repeated application should ensure that the steady state process error will reduce to zero. The closed loop transfer function can be examined to determine the steady state error of the

system. The closed loop transfer function of the block diagram in Figure 17 is shown in Equation 11 and reduces to Equation 12.

$$\frac{p_i}{p_{ref}} = \frac{\frac{g_C g_P}{1 - z^{-1}}}{1 + \frac{g_C g_P z^{-1}}{1 - z^{-1}}}$$

Equation 11

$$\frac{p_i}{p_{ref}} = \frac{g_C g_P z}{z - 1 + g_C g_P}$$

Equation 12

Where:

p_i= *part shape for the* i^{th} *iteration*

p_{ref}= *reference part shape*

g_p= *plant matrix*

g_c= *controller matrix*

Changes to the target shape can be approximated as a unit step input. The response of the closed loop transfer function, in the steady state, to a unit step input can be determined by multiplying the transfer function by a step input (z-1) and taking the value of the closed loop transfer function as z approaches unity. This can be represented by Equation 13.

$$\lim_{z\to 1}(z-1)\left(\frac{g_C g_P z}{z-1+g_C g_P}\right)\left(\frac{z}{z-1}\right)=1$$

Equation 13

The value produced is unity. This means that the desired output will match the input and should result in no steady state error. This behavior stems from the "integrating" effect of the shape control algorithm which adds the error of the last part formed to the error from all previous parts formed and accounts for them in successive iterations. The algorithms used take the general form of a proportional – integrating controller (PI) which has been shown by Siu [17] to be the optimal controller form.

3.1.9 Variance Amplification

Random variation is inherent to all manufacturing processes. This is the result of system noises or disturbances (noise and disturbance will be used interchangeably in this thesis). How well the controller responds to disturbance input is an important consideration. Disturbances are usually modeled as additive inputs and can affect the system dynamics at every step in the process. Common sources of disturbance in the stretch forming process are die setup, measurement, forming dynamics, part mishandling, and material variation. Noise sources and their effects are discussed in greater detail in section 4.5. An example of a disturbance input during the die setup process is shown in Figure 20.

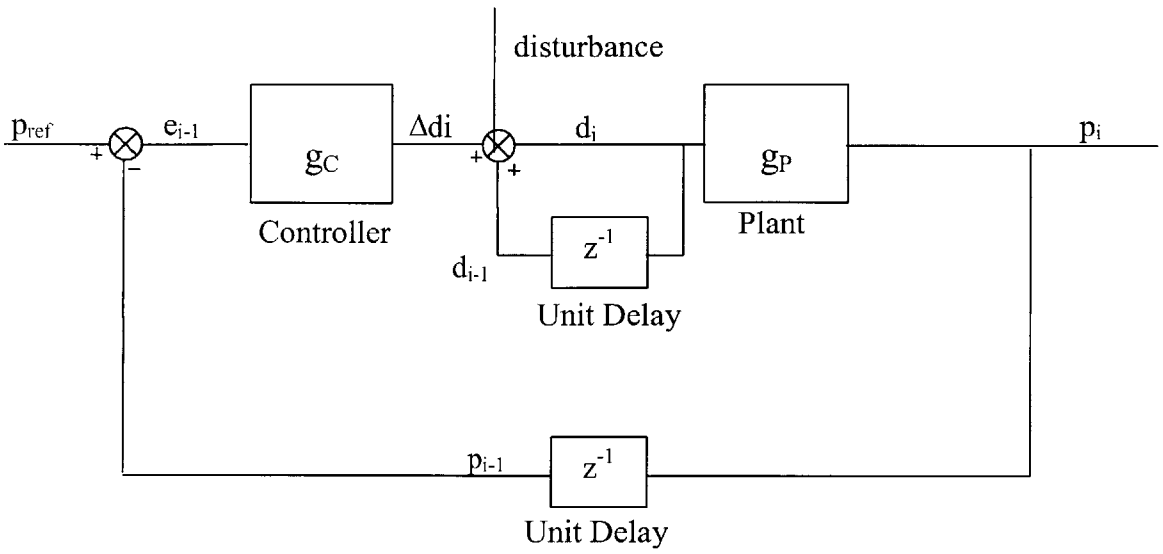

Figure 20: Block diagram modeling disturbance input at die setup

Diagram from Pi [10]

Disturbances can be of different types (random, systematic, and/or periodic). Pi [10] analyzes the steady state effects of several disturbance inputs and shows that additive disturbances will not affect the steady state value of the system output.

Process disturbances can be correlated or uncorrelated. Siu [17] analyzed the output variation resulting from correlated and uncorrelated disturbance inputs. Stretch forming operations are dominated by uncorrelated noise so only these will effects will be discussed further (see Siu [17] for variation effects from correlated noise). He determined that applying CtC control to a manufacturing process could increase output variation in the presence of uncorrelated noise. The variance amplification is the result of the one cycle delay in the control structure. For example, die changes (implemented during the current cycle) are partially based on noise observed in the previous cycle. This noise is assumed to be a normal identically distributed independent (NIDI) process input with a mean (μ) and a variance ($\sigma^{2)}$. The controller attempts to compensate for this noise by adjusting the die shape for the next forming cycle. However, this noise may or may not be present in this cycle at the same amplitudes as it was during the previous cycle. In effect, this shape "correction" will have the unintended consequence of adding variation to the process. In other words, the effect of disturbances can be amplified as a result of

using CtC control. The variance amplification plots shown in Figure 21 illustrate the effect of different loop gain values on the output variation.

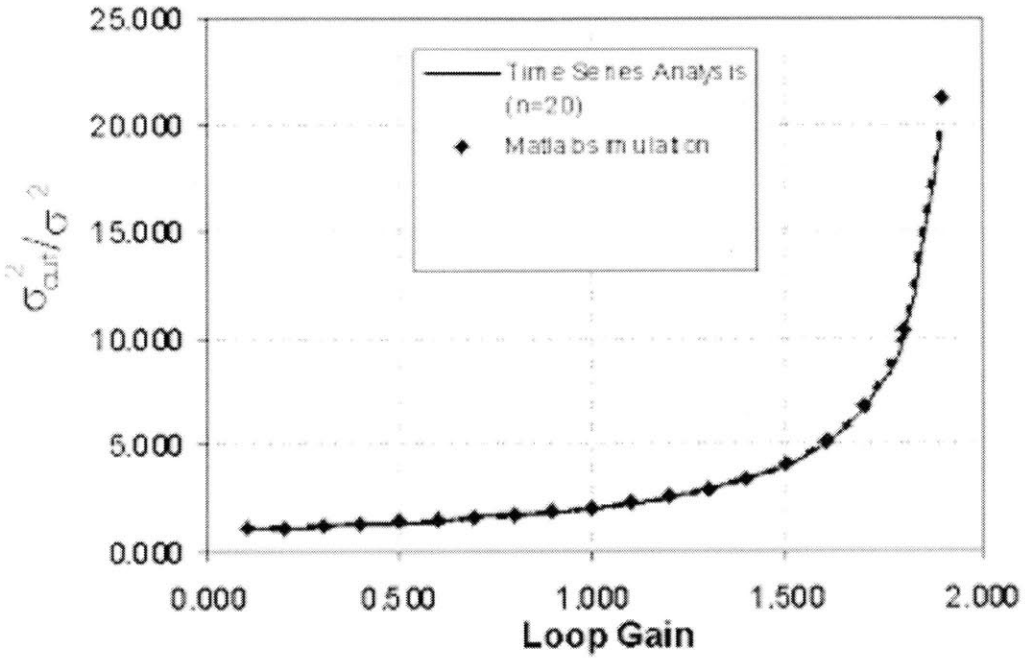

Figure 21: Variance Amplification for uncorrelated noise in CL systems

The variance ratio changes over a range of loop gains. Lower loop gain values result in less variance amplification. The variance ratio is the variance of the output divided by the variance of the input. Diagram from Rzepniewski [18]

The process output variance ($\sigma_{y_n}{}^2$) can be determined by taking the disturbance input $d_i \sim (0, \sigma^2)$ into account. This is shown in Equation 14.

$$\begin{aligned}
\sigma_{y_n}{}^2 &= \sigma^2 + (-K_p K_c)^2 \cdot \left[\sum_{i=1}^{n-1} \sigma^2 \cdot (1 - K_p K_c)^{2(n-i-1)} \right] \\
&= \sigma^2 \cdot \left\{ 1 + (-K_p K_c)^2 \cdot \left[\sum_{i=1}^{n-1} (1 - K_p K_c)^{2(n-i-1)} \right] \right\} \\
&= \sigma^2 \cdot \left\{ 1 + (-K_p K_c)^2 \cdot \frac{1 - (1 - K_p K_c)^{2(n-1)}}{K_p K_c \cdot (2 - K_p K_c)} \right\} \\
&= \sigma^2 \cdot \left\{ 1 + K_p K_c \cdot \frac{1 - (1 - K_p K_c)^{2(n-1)}}{2 - K_p K_c} \right\}
\end{aligned}$$

Equation 14

The ratio between the variance of the disturbance (σ^2) and the variance of the output ($\sigma_{y_n}{}^2$) is isolated in Equation 15.

$$\frac{\sigma_{y_n}{}^2}{\sigma^2} = 1 + K_p K_c \cdot \frac{1 - (1 - K_p K_c)^{2(n-1)}}{2 - K_p K_c}$$

Equation 15

We observed previously that the system will converge fastest if the loop gain ($K_p K_c$) is unity. Substituting $K_p K_c = 1$ into Equation 15 we find that the resulting variance ratio $\sigma_{y_n}{}^2 / \sigma^2 = 2$. This means that the preferred implementation of CtC control ($K_p K_c = 1$) will have the effect of doubling the process variance. Fortunately, it was also shown that the integral controller reduced the steady state error to zero. Experiments are presented in Chapter 5 that determine if the benefits of zero mean error outweigh the drawbacks of CtC variance amplification.

3.2 Cycle to Cycle Control Algorithms

The generic CtC control framework developed in the previous sections is well suited to the stretch forming process. What is required is a process model that adequately simulates the specific process dynamics of sheet metal stretch forming. The greatest obstacle is designing the MIMO equivalent of the ideal SISO controller described previously. MIMO processes such as reconfigurable die stretch forming are particularly difficult to model due to the output coupling. Coupling describes the influence an individual die location will have on the shape of adjacent part locations. In particular, this refers to the effect that changing a single shape input will have on the local shape output. This is shown graphically in Figure 22.

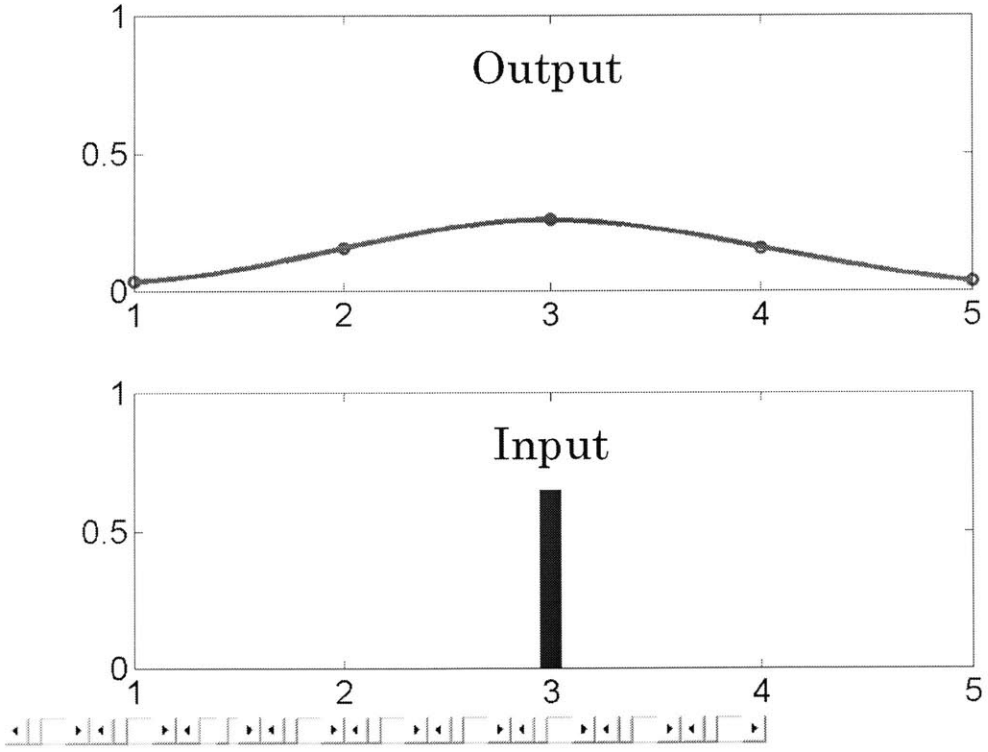

Figure 22: Stretch forming process coupling

Note that an individual input can have an effect over a broad area of local outputs. Diagram from Rzepniewski [19]

Several control algorithms have been developed to model the stretch forming process. Norfleet [8] classified the various shape control algorithms according to the table in Figure 23.

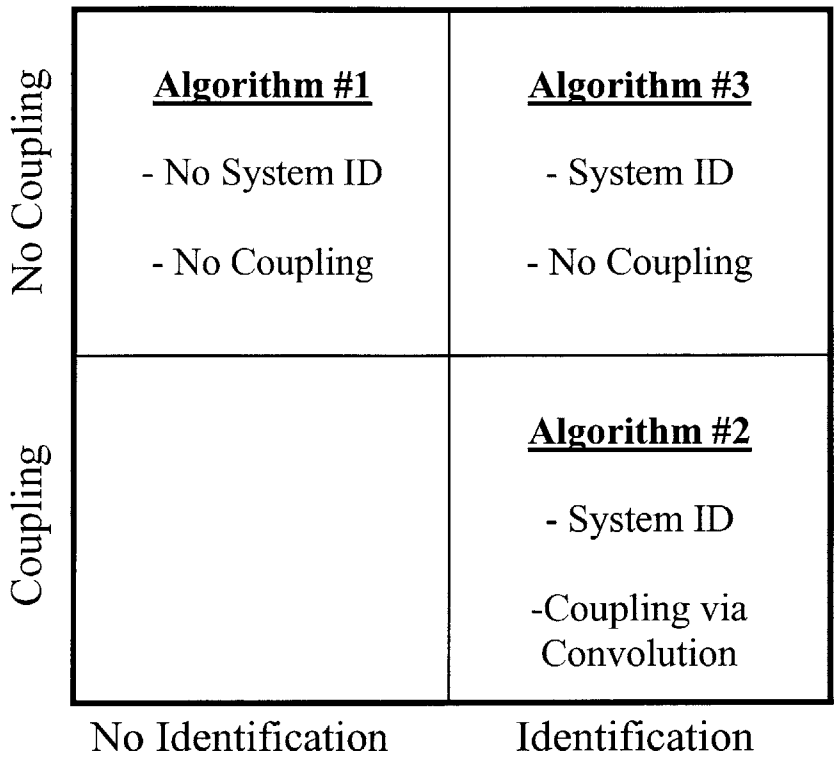

Figure 23: Table of different algorithms used for shape control

Diagram from Norfleet [8]

Further details regarding these algorithms can be viewed in Norfleet [8]. Algorithm #1 was initially developed by Webb [13]. It is the simplest algorithm to implement since it does not require a system ID or account for process coupling. Unfortunately, this lack of sophistication was shown to result in poor performance and long settling times due to the inaccurate process model. This algorithm was implemented by taking the error from the prior part and then incrementing the die by same amount. This can be viewed as a cycle to cycle control algorithm where the controller gain is set to unity. The next die is calculated by moving each pin at location (x,y) by the part error at the same location only.

Algorithm #2, also known as the Differential Transfer Function (DTF), was developed by Webb [14], Osterhout [15] and Valjavec [6] to address several areas of concern with Algorithm #1. Algorithm #2 accounts for the forming dynamics between different locations on the part and die. This is represented in the form of a system identification (an estimate of the plant matrix). This system identification is then used to calculate appropriate controller gains to achieve the most desirable system response. As a result, Algorithm #2 requires fewer cycles to reach a desired part shape. Algorithm #2 accounts for process coupling via convolution. This is accomplished through the introduction of the Fourier transform. The algorithm is applied to part and die representations in the frequency domain. A change to a single frequency of in the part or die can affect multiple points in the adjacent part or die surface. Valjavec [6] performed an experimental analysis of algorithm #2 and showed that it performs better than Algorithm #1. Unfortunately, Valjavec [6] and Norfleet [8] also showed that this algorithm is more sensitive to noise as well as being more complicated to implement than Algorithm #1.

This research is primarily interested in Algorithm #3, also known as the Spatial Coordinate Algorithm (SCA). More information on Algorithms #1 and #2 can be found in Valjavec [6], Norfleet [8], and Pi [10]. Experimental results from Algorithms #1 and #2 are presented in Appendix B.

3.3 Spatial Coordinate Algorithm (SCA)

SCA is a simplified version of the DTF. The major distinction is that SCA performs a system identification without the use of the Fourier transform operation. The SCA block diagram is shown in Figure 24.

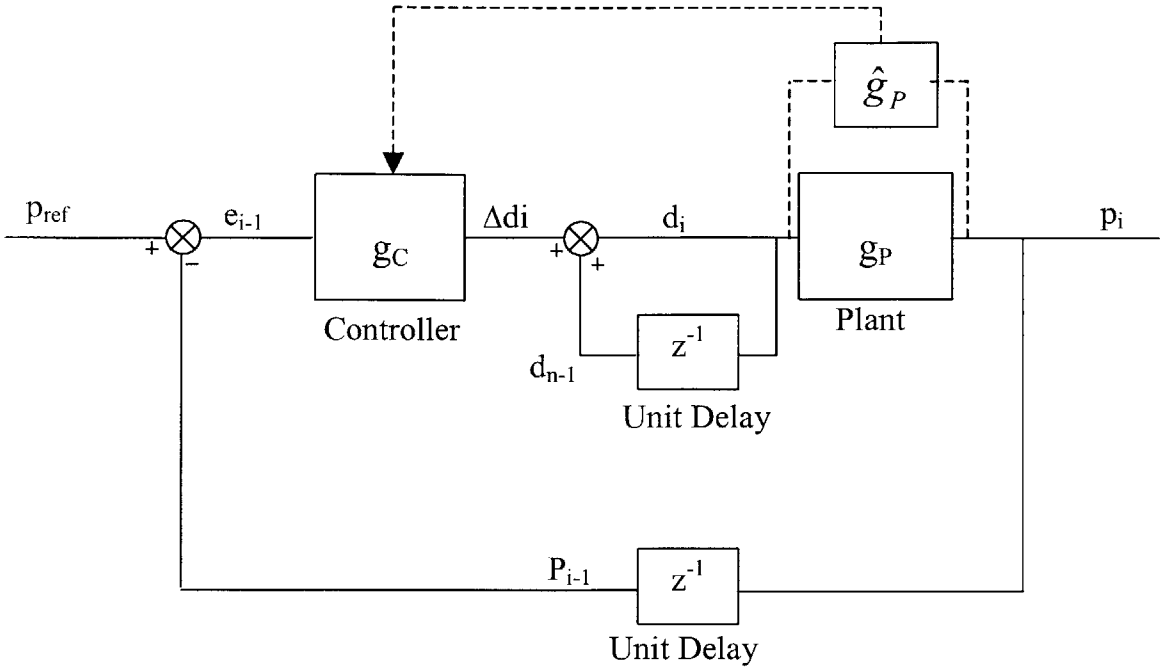

Figure 24: Block diagram for Algorithm #3 - SCA

The SCA performs an estimate of the plant gain matrix, and sets the controller gains so that the overall loop gain is unity. All operations are done in the spatial domain. Diagram from Pi [10]

The spatial coordinate algorithm is implemented by using Equation 16 and Equation 17.

$$\underline{d}_i = \underline{d}_{i-1} + G_C(\underline{p}_{ref} - \underline{p}_{i-1})$$

Equation 16

$$\underset{(MN,1)}{\begin{bmatrix} {}_1d_i \\ {}_2d_i \\ \vdots \\ {}_{MN}d_i \end{bmatrix}} = \underset{(MN,1)}{\begin{bmatrix} {}_1d_{i-1} \\ {}_2d_{i-1} \\ \vdots \\ {}_{MN}d_{i-1} \end{bmatrix}} + \underset{(MN,MN)}{\begin{bmatrix} {}_1g_C & 0 & 0 & 0 \\ 0 & {}_2g_C & 0 & 0 \\ 0 & 0 & \ddots & 0 \\ 0 & 0 & 0 & {}_{MN}g_C \end{bmatrix}} x \left(\underset{(MN,1)}{\begin{bmatrix} {}_1p_{ref} \\ {}_2p_{ref} \\ \vdots \\ {}_{MN}p_{ref} \end{bmatrix}} - \underset{(MN,1)}{\begin{bmatrix} {}_1p_{i-1} \\ {}_2p_{i-1} \\ \vdots \\ {}_{MN}p_{i-1} \end{bmatrix}} \right)$$

Equation 17

The estimate of the plant matrix is determined by Equation 18.

$$G_P = \frac{P_2 - P_1}{D_2 - D_1}$$

Equation 18

As mentioned in Section 3.1.5, the controller gain is set so that the overall loop gain is unity. As a result, the SCA controller is defined by Equation 19.

$$G_C = G_P^{-1} = \frac{D_2 - D_1}{P_2 - P_1}$$

Equation 19

The spatial coordinate algorithm represents a compromise between complexity and accuracy. Recall from Section 3.1.5 that the diagonal of the gain matrix corresponds to the effect that each point on the die has on the corresponding part location. The off-diagonal terms are a measure of the degree of coupling between adjacent die and part locations. Observation of Equation 17 shows that the controller gain matrix (g_c) is purely diagonal and that all off-diagonal terms are zero. This means that SCA does not account for process coupling. It does, however, account for springback as a result of the stretch forming process through the system identification process.

3.4 Coupling Shape Coefficients (CSC)

The Fourier transform utilized in the DTF has the effect of coupling all of the outputs to all of the inputs. The SCA disregards coupling altogether. Rzepniewski [19] noted that the actual form of the coupling should approximate a Gaussian distribution. As applied to discrete die sheet metal forming, this means that a pin (input) will exhibit strong coupling to the local part areas (outputs) only. The degree of coupling will diminish as the distance from the input increases. This is intuitively a more accurate reflection of the process dynamics. Simulated results have shown that the Gaussian model, or Coupling Shape Coefficients (CSC), offers more accurate predictions of the output for a given input.

3.5 Summary

This chapter examined several forms of open and closed loop manufacturing process control methods. The basis of CtC control was presented. It was shown that CtC control offered the ability to reduce process error to zero at the expense of an amplification of the variance. DTF, SCA, and CSC control algorithms were introduced. It was shown that the SCA offered similar error reduction capabilities as the DTF without the complexity and noise sensitivity. The CSC algorithm appears to offer the most accurate process model.

CHAPTER

4

IMPLEMENTATION OF FORMING METHODS

The forming methods discussed in the previous chapter can be used to control the reconfigurable die stretch forming press. It is possible to analyze the performance of each control method if we produce a sample production run of parts. Each production run will have inherent trends and variations. We are primarily interested in the *mean shift* and *variance* of the production run. The mean shift describes the accuracy of the process. The variance describes the consistency of the process. This chapter will address how we will critique the choice of forming method based on the process mean shift and variance. Possible system noises/disturbances will be presented and quantified if possible. Two open loop forming methods (Fixed Die and Reconfigurable Die) will be evaluated by calculating the process mean shift and variance.

4.1 Part Quality Evaluation

This chapter compares the performance of several forming methods. The process performance is the net shape difference between the target part shape and the actual part shape, or the part error. Each part must be measured and registered, with respect to the target shape, in order to determine the part error.

4.2 Part measurement

The surface of each part is measured after being formed. We use a Brown and Sharpe MicroVal PFx Coordinate Measuring Machine (CMM) although any device that can measure surfaces accurately in the Cartesian coordinate system is acceptable. The CMM, shown in Figure 25, can measure the part surface on a user-defined grid. The resultant measurement data is represented as a cloud of points.

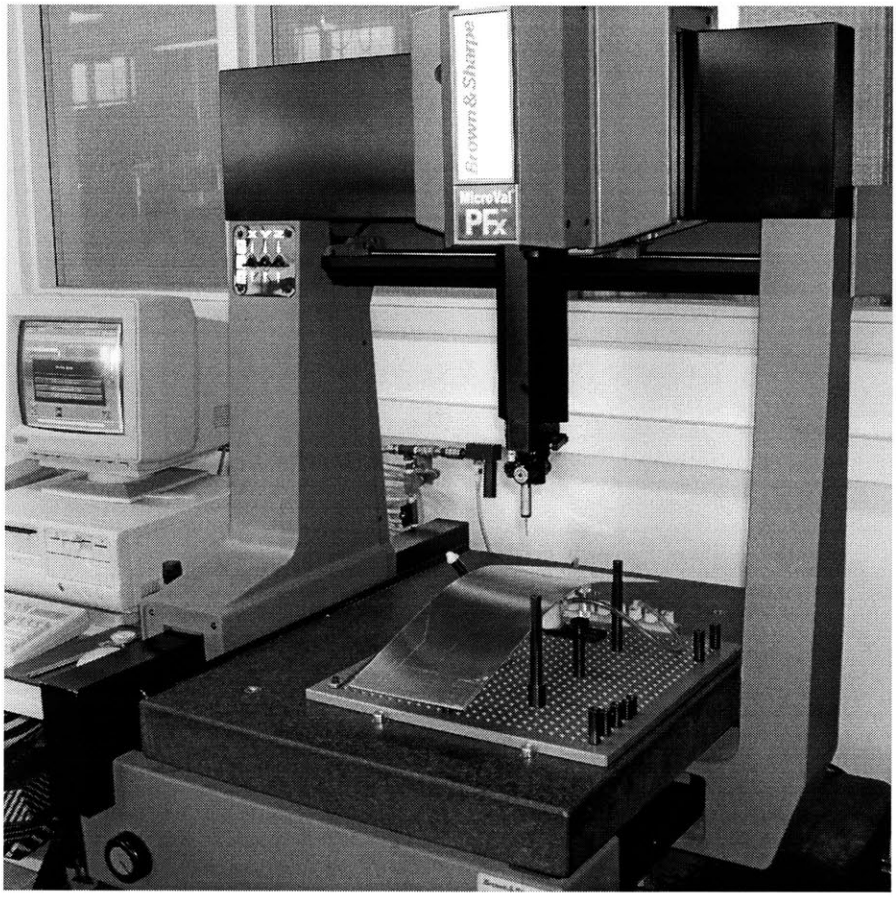

Figure 25: Brown and Sharpe MicroVal PFx CMM used to measure formed parts.

A center point for each part is designated using a small punch mounted on the forming press (see Figure 26). This is done before the part is removed from the press to

ensure that the center point is identical, with respect to the die, on all parts. The CMM uses this center point as a reference for all other measured points.

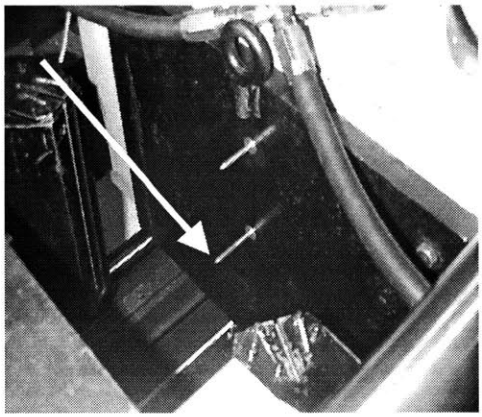

Figure 26: Punch used to create reference mark (center point) on formed parts.

Photo from Pi [10]

It is very unlikely that the exact locations of the data points measured by the CMM are identical from part to part. As a result, some interpolation is necessary. The CMM is instructed to take part measurements on a much finer scale than the die. Interpolation is then used to determine the points that can be compared appropriately. This procedure is shown in Figure 27. A variety of interpolation methods have been used in the past, including bi-cubic spline interpolation, and linear interpolation. The benefit of some of the more elaborate forms of surface fitting includes "smoothing" the data. However, different surface fitting techniques do not alter the part representation significantly. Advances in measurement techniques, such as Accordion Fringe Interferometry, might allow for quicker and more accurate measurements of the part [6]. They may also allow better surface fitting techniques and estimation.

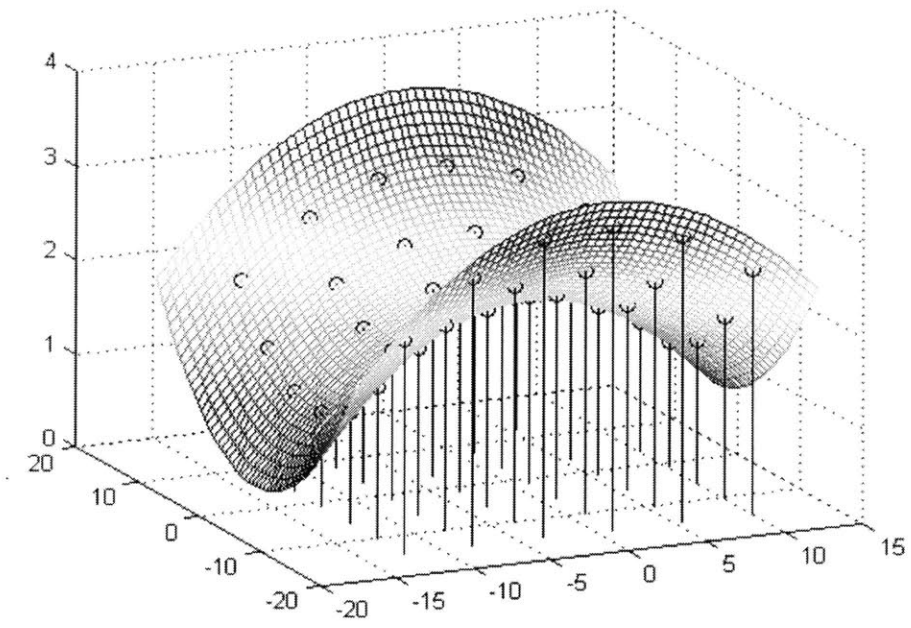

Figure 27: Figure of a part representation

Points corresponding to a die are evenly spaced along both the X and Y axes. Diagram from Norfleet [8]

4.2.1 Part Registration

In Figure 27, it is assumed that the part has been oriented and aligned properly to a standard. Due to variation and uncertainties in the forming process, it is very unlikely that the part can be placed on the CMM in such a way that the same locations are measured each time. A process called registration is used to orient the parts so they can be more accurately compared. The parts formed at MIT by Valjavec [6], Pi [10], and this author have one reference point that is close to the center of the surface. The Z coordinate values are all shifted after the part has been measured so that the "center" of the reference part and formed part match. The registration method used in this research includes an iterative approach to part registration. This is done by adjusting the part along the Z axis, and then rotating the part along the X and Y axes until the RMS (root mean square) error is at a minimum. Since registration routine searches through a finite orientation range, care must be taken that the orientation of the part which will result in the least error is

placed within that range during the measurement process. Once the angles of rotation along different axes have been determined, the points on the grid of the part are then calculated and reformed in the new configuration. This new part is then considered registered, with respect to the die, and the reference part. Further details can be found in Valjavec [6] and Pi [10].

Other implementations of the part registration procedure involve 2 or even 3 reference points. Each reference point limits more degrees of freedom, and allows a quicker and potentially more accurate registration routine [7].

4.3 Error Calculation

The CMM outputs a 30 x 35, three-dimensional grid of part elevations in X, Y, and Z coordinates. This grid is on a scale approximately 3 times as fine as the grid of forming pins (10 x 11). The controller only has a resolution equal to the resolution of the forming pins (which are ½" by ½"). Therefore, it's necessary to interpolate the part profile obtained from the CMM onto a courser grid. This "re-gridding" is also done with the reference shape since it is initially created on a 46 x 51 grid. This allows us to compare "apples to apples". The part error is calculated by subtracting the part shape elevations from the reference shape elevations as shown in Equation 20.

$$e_i = p_{ref} - p_i$$

Equation 20

Where:

e_i = *Part error*

p_{ref} = *Matrix of target shape elevations*

p_i = *Matrix of part shape elevations*

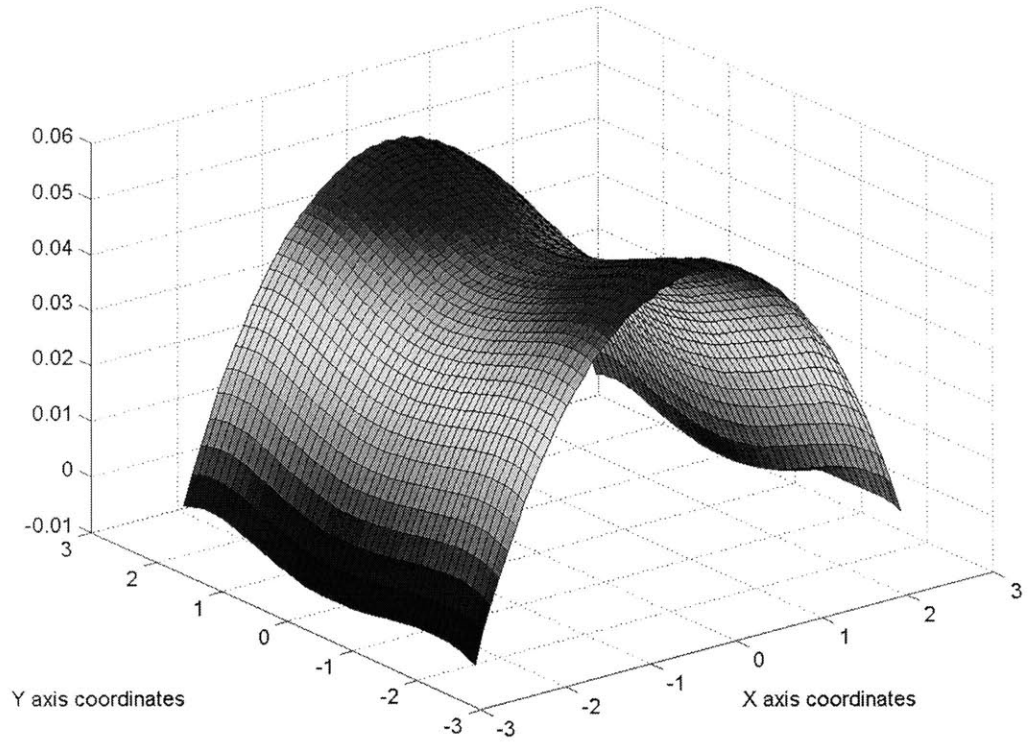

Figure 28: Sample error plot for a part

Diagram from Pi [10]

The resulting net shape error, shown in Figure 28, is analyzed in several ways. We are mainly concerned with Maximum Error, Root Mean Square Error, and Mean Error. These three measurements are individually and collectively useful for analyzing the trends of the data.

4.3.1 Maximum Error

The maximum error reflects the part accuracy and is determined by searching the error matrix for the entry of greatest positive or negative magnitude. Maximum error represents the worse case error of the part.

4.3.2 Root Mean Square Error

Root mean square (RMS), error is a quantitative measure of overall part quality. This measurement describes how well the part conforms to the target shape as a whole. This indicates the extent to which the maximum error is descriptive of the entire part. In other words, the RMS error reflects the part precision.

4.3.3 Mean Error

The RMS error is an adequate representation of the overall part quality. However, the formula requires squaring of the error term. This means that all values for RMS error will be positive. We can't tell if the part is being over- or under-formed from observing the RMS error. The Mean, or average, error takes the mean value of the error matrix. The mean error is a more useful indicator of the overall part quality since it carries information about the accuracy *and* precision of the part.

4.4 Part Quality Threshold Criteria

Maximum error is used as the criteria for determining part acceptability. This stems from the interests of the primary sponsor of this project. The aircraft industry is interested in using the reconfigurable die stretch forming machine in a production line. Their main concern is that the parts produced are "good enough". RMS and Mean Error values describe the overall quality of the parts. They don't readily lend themselves to design tolerances and other manufacturing assembly concerns since they don't bound the part error. Although this maximum part error does not give a measure of the overall part quality, it is of particular interest in the aerospace industry and other applications where a threshold level of error must be met for all points on the part surface.

Valjavec [6] stopped forming parts once the maximum part error went below 0.01". This was designated as the "threshold" level because this was the estimate of the process noise.

4.5 Process Noise/Disturbances

Random variation is inherent in all manufacturing processes. There are also additional noises and disturbances resulting from unwanted system inputs. These usually have an assignable cause which can be identified and reduced or eliminated. There are five major sources of noise/disturbance in the forming process. Figure 29 details a basic representation of the disturbance inputs.

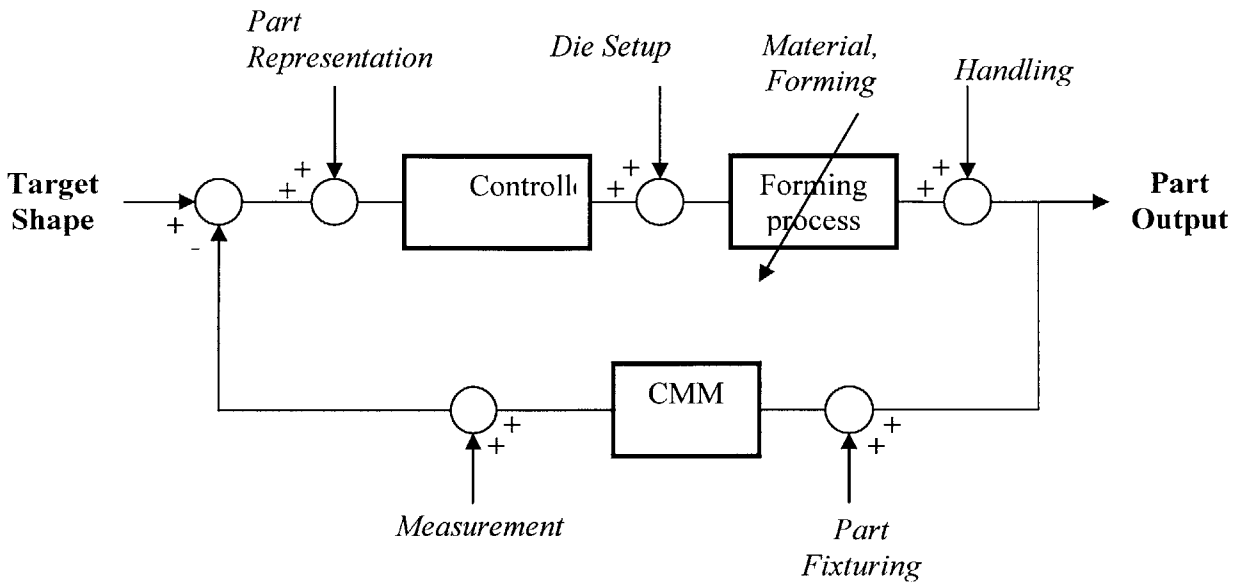

Figure 29: Noise inputs into control loop

Quantification of the disturbances is attempted in subsequent sections. Unfortunately, it is often not possible to totally segregate the effects of each disturbance. This is noted where applicable.

4.5.1 Die Setup Noise

The controller instructs the press the set up a specific die shape. The die setup process is not purely deterministic. Four mechanical connections must be made in series to move each die pin to the proper location. These connections are detailed in Figure 30.

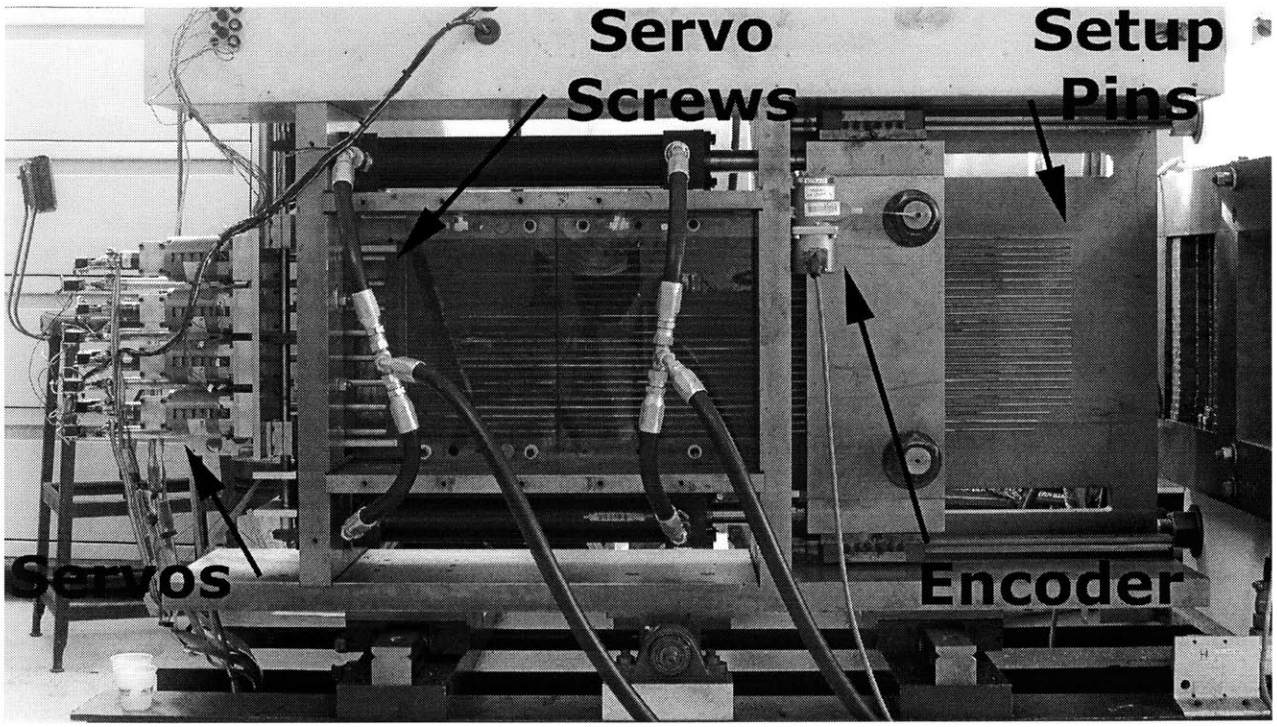

Figure 30: Die setup mechanism

The Servos cause the Servo Screws to move the Setup Pins to the correct elevations. The Setup Pins, whose motion is controlled by the Encoder, adjust the elevation of the Forming Pins to create the die shape.

There is uncertainty associated with each connection. The final die shape is the sum of the controller input and the cascading uncertainty in the die setup mechanism. These disturbances have been quantified using ten dies from a sample production run. A Starrett digital micrometer (with a published accuracy of 0.0005") was used to measure the actual forming pin elevations immediately following the die setup procedure. This actual die shape was compared to the requested die shape. The die setup error is defined in the same fashion as the part error. As before, we are primarily interested in the mean error. This is detailed in Figure 31.

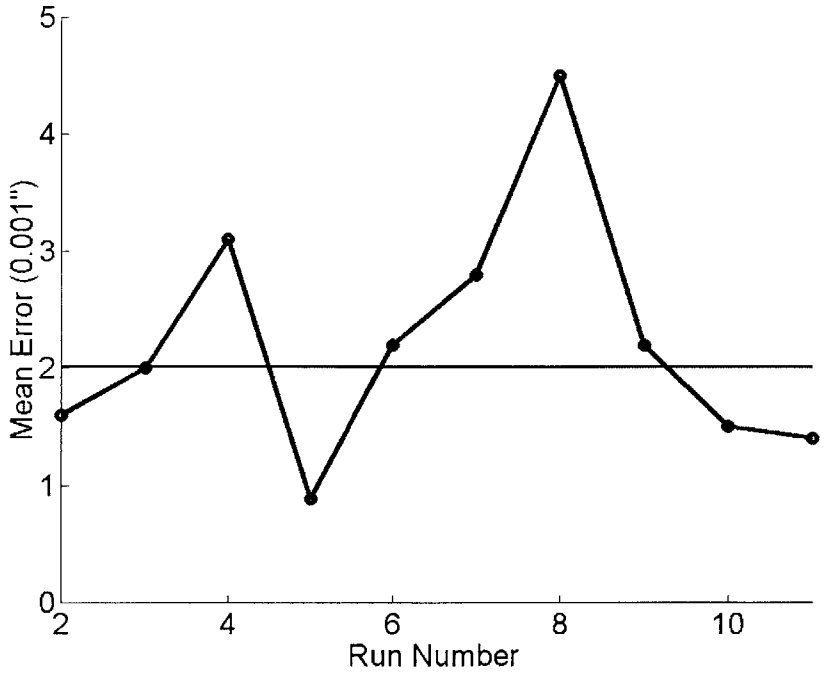

Figure 31: Die setup mean error

We find the average of the mean error values to be 2.02 mils (a mil is 0.001 inches). The process assumes that the die is projected to the specified elevation. The part is wrapped based on the calculated die position. There is no knowledge of the actual die position. This discrepancy introduces error into the formed shape. The process variance is defined by Equation 21 [12].

$$\hat{\sigma}^2 = \left(\frac{S}{c_4}\right)^2$$

Equation 21

And:

$$c_4 = \left(\frac{2}{n-1}\right)^{1/2} \frac{\Gamma(n/2)}{\Gamma[(n-1)/2]}$$

Equation 22

Where:

$\hat{\sigma}^2$ = *Estimate of the process variance*

S = *Sample standard deviation*

n = *number of samples in production run*

c_4 *is a statistical adjusting factor*

S	1.04 mils
N	10
C_4	0.9727
$\hat{\sigma}^2$	1.14 mils^2

Table 1: Die setup variance

Applying Equation 21, the die setup variance is found to be 1.14 mils^2.

4.5.2 Material/Forming Noise

Several types of disturbance are input into this area of the system. Material variation and interpolator memory affect the part shape during the forming process. The stretch force is based on theoretical calculations that describe the material's strain state under an applied load. These calculations are based on a specific cross-sectional area. Any variation will result in a change in the strain state, and consequently, the formed part. The interpolator is another source of system noise. The interpolator will develop a memory over time (permanent impressions in the interpolator material). This deformation in the interpolator adds noise to the part shape.

4.5.3 Part Handling Noise

There is also possible disturbance added to the process due to mishandling when the formed part is removed from the press. The material clamps don't allow for much part clearance. This causes very slight part distortion. The loads placed on the part are relatively far from the area of interest so the distortion is very minimal. The effects of these disturbances have not been quantified individually since they are difficult to segregate.

4.5.4 Part Fixturing Noise

The part is measured on the CMM after being formed. A fixturing device is used to hold the part securely. This fixture utilizes two vacuum clamps and two support posts. The vacuum clamps pull the part downwards from the part center. The support posts push upwards from the part ends. The function of the vacuum clamps is to secure the part to the CMM table. The function of the support posts is to support the weight of the part and resist any deflection caused by the CMM probe. Ideally, the part should see no deflection from the posts beyond that required to support the weight of the part. If the support posts are raised too high the part shape will be deflected upwards. If the posts are too low the part shape will deflect under its own weight and CMM probe will deflect it further (upon impact) and give a distorted measurement. These features are shown in Figure 32.

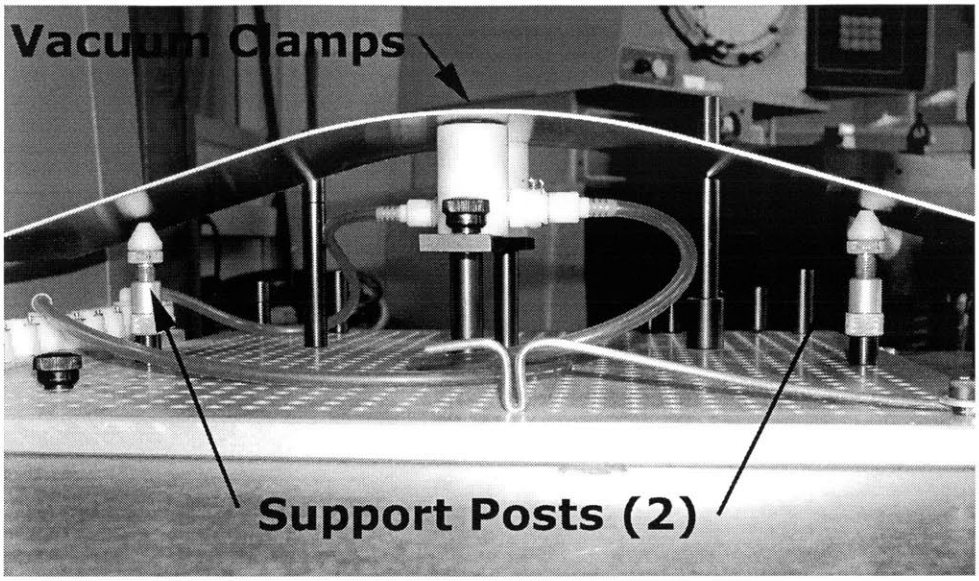

Figure 32: CMM fixturing device

The fixturing error is influenced by the measurement noise. It is possible to segregate these two sources (discussed below). Quantification of the fixturing noise has only been carried out in tandem with the measurement noise.

4.5.5 Measurement Noise

The measurement process adds noise of its own. This noise originates from the CMM's sensors and actuators. The Brown and Sharpe CMM used in the experiments has a listed standard deviation of 0.0001".

4.5.6 Part Representation Noise

Part representation noise includes disturbances input into the system as a result of computer manipulation of the part model. The part model and target shapes are discrete depictions of a continuous shape. The level of discreteness varies between the control algorithms, die, and CMM. Interpolation, splines, and other methods are used to bridge these differences. This uncertainty is difficult to individually quantify and has not yet been done.

Pi [10] determined that the combined noise input from fixturing, measurement, and registration was 0.0015". This value was found by refixturing, measuring, and registering a single part three times.

4.6 Fixed Die Performance

Utilizing a reconfigurable die in the stretch forming process adds another source of system noise. This can be quantified by comparing the part quality of a fixed die production run to the part quality of a reconfigurable die production run. We want to benchmark the performance of this process in order to compare other tools and control methods. The process can be characterized by evaluating the process centering (mean shift) and variance of the mean error of a sample production run.

4.6.1 Fixed Die Parameters

We can use the discrete die described previously as a fixed die. This is done by first setting up a discrete die shape and then clamping the bundle of discrete pins in place. This clamping force effectively secures each pin in place and resists any individual or collective pin motion. This fixed die is used to form a sample production run. The pin bundle remains clamped throughout the run to ensure no relative pin motion.

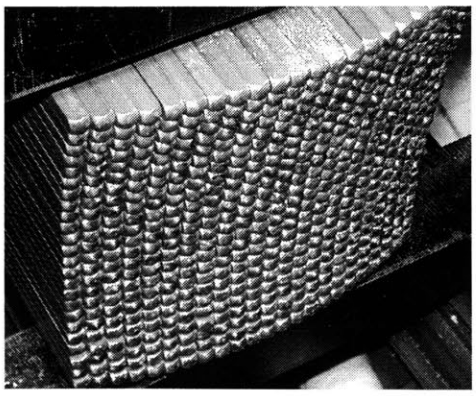

Figure 33: Forming surface of reconfigurable die

The die shape selected for this production run has been used previously to form parts that met the part quality criteria (i.e. maximum part error < 0.01"). Identical forming parameters were also used. These are detailed in Table 2.

Parameter	Value
Pin size	0.5 inch
Stretch Force	6125 lbs.
Part Material	Al 2024-O, 19.5 x 5.5 x 0.063 inches
Final part footprint	4.5 x 5.0 inches
Force trajectory	Pre-stretch, wrap, no post stretch
Control mode	Force control
Interpolator	Elvax 360 (0.535 in. thick) covered with two layers of Teflon
Target Shape	10.65" radius reference cylinder

Table 2: Machine parameters used to form part production run

These parameters are used for all forming runs in this research.

4.6.2 Fixed Die Process Results

Ten parts were formed using the parameters detailed in Table 2. The Maximum, RMS, and Mean errors were calculated for each part using the equations described previously. The results are plotted in Figure 34.

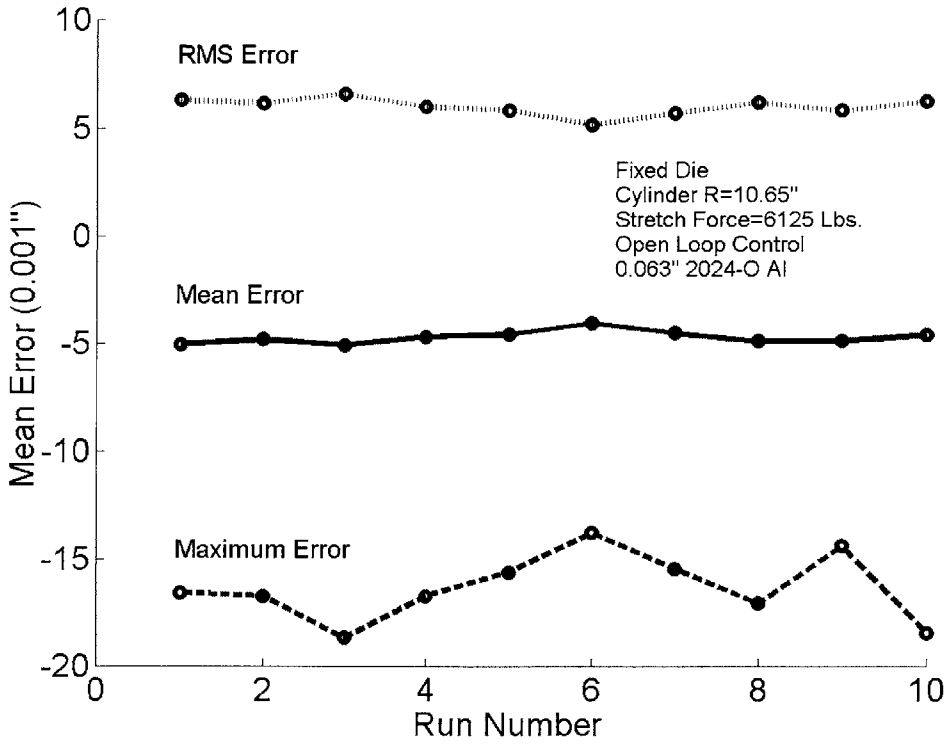

Figure 34: Fixed die production run errors

4.6.3 Fixed Die Process Centering

The mean error is the difference between the formed shape and the target shape on a part-by-part basis. The average of the mean error over many parts is a measure of how "centered" the process is. Ideally, we wish to observe the stretch forming process centered about an average mean error of zero inches.

The mean error of the process is evaluated using the equations detailed previously. This is shown in greater detail in Figure 35.

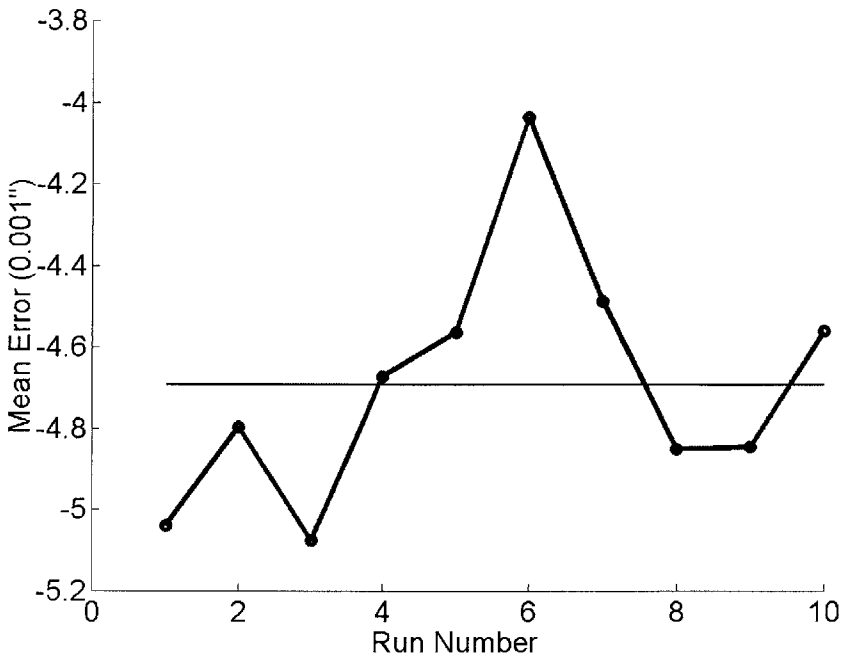

Figure 35: Fixed die production run mean error

The data shows that the mean error of the process is centered about -4.69 mils. This deviation from the process center, or mean shift, is a common occurrence in all open loop processes. Virtually any alteration in the process inputs will cause a mean shift. Non-standard operating procedures, material change, and changes in operator input are common. The size of the mean shift will depend on the process sensitivity to the input(s) that are altered.

4.6.4 Fixed Die Variance

Using Equation 21 we find the results detailed in Table 3:

S	0.30 mils
n	10
C_4	0.973
$\hat{\sigma}^2$	0.098 $mils^2$

Table 3: Fixed die production run process variance

As the table shows, the estimated process variance ($\hat{\sigma}^2$) is found to be 0.098 $mils^2$.

4.7 Reconfigurable Die Performance

We want to evaluate the suitability of replacing a monolithic die with a reconfigurable die in a job shop environment. Typically, a job shop will set up a die and form a small run of parts. This run is often no more then a single part. The die will then be removed and the cycle repeated with another die for a different part (it is assumed that the accuracy of the monolithic dies have already been deemed acceptable). Replacing the monolithic die with a reconfigurable die would reduce costs incurred from die manufacture and setup and eliminate die storage costs (which can be significant for large dies).

The performance of the reconfigurable die in a job shop environment can be benchmarked by simulating the die set-up process. The part errors can be analyzed and compared to the part errors from the production run utilizing the fixed die.

4.7.1 Reconfigurable Die Parameters

The fixed die shape experiments are repeated under identical conditions, except that the die shape is reset between each forming cycle. In this way, any additional variation caused by the die setup procedure can be identified.

4.7.2 Reconfigurable Die Process Results

Eight parts were formed using the parameters detailed in Table 2. The Maximum, RMS, and Mean errors were calculated for each part using the equations described previously. The results are plotted in Figure 36.

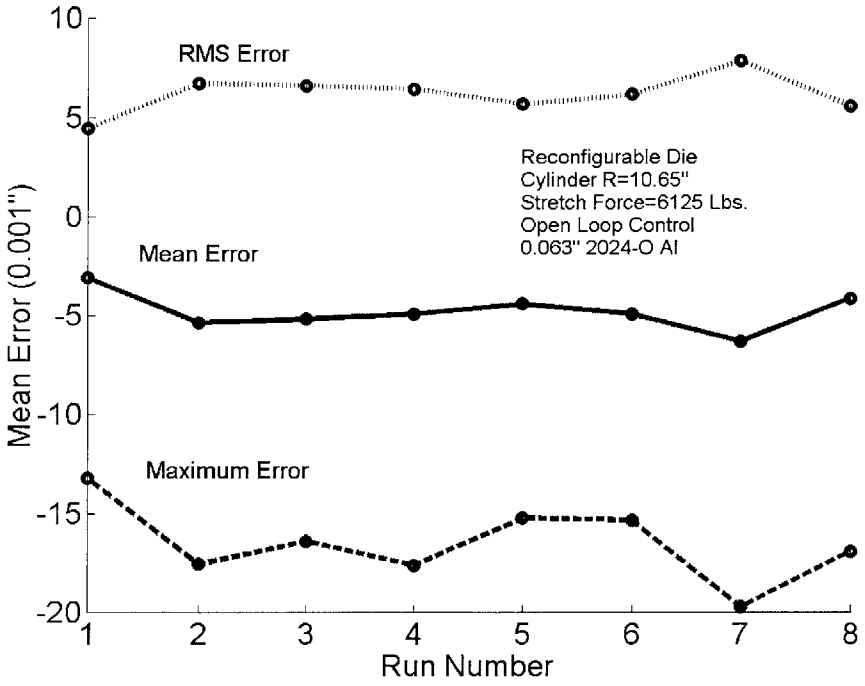

Figure 36: Reconfigurable die production run errors

4.7.3 Reconfigurable Die Process Centering

The mean error of the process is evaluated using the procedures detailed previously. The data shows that the mean error of the process is centered about -4.79 mils. This is shown in greater detail in Figure 37.

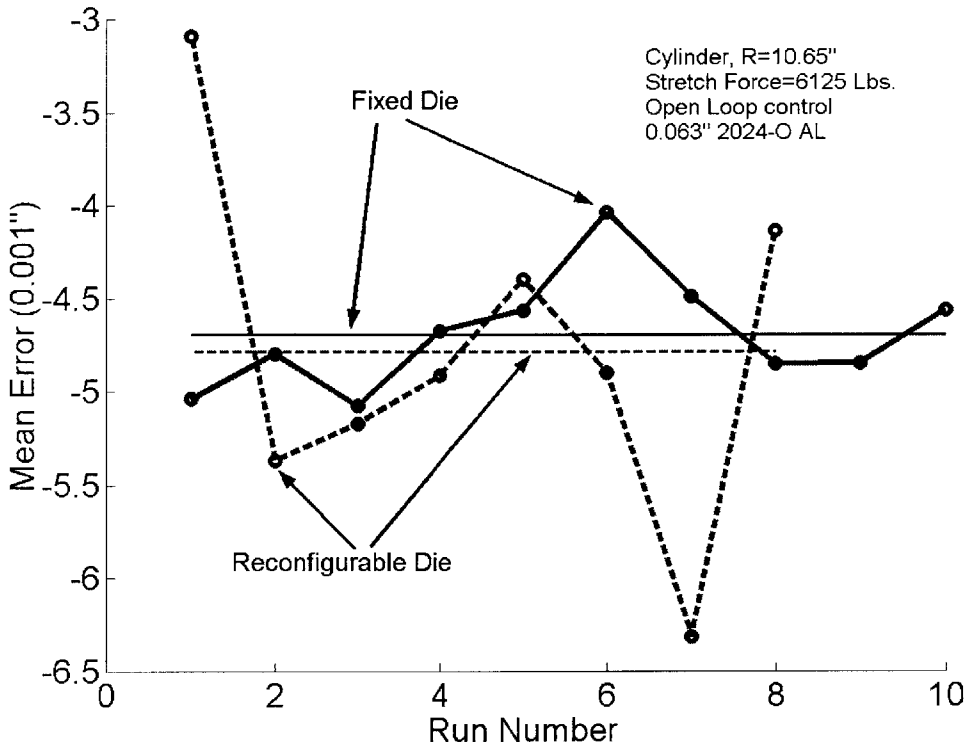

Figure 37: Reconfigurable die production run mean error

The introduction of the die setup process into the forming cycle shifted the process mean further off center. However, the shift is not considerably great and no definite conclusions can be drawn considering the magnitude of the process variance.

4.7.4 Reconfigurable Die Process Variance

The process variance of this production run is calculated using Equation 21 and detailed in Table 4.

S	0.95 mils
n	8
C_4	0.9650
$\hat{\sigma}^2$	0.97 mils^2

Table 4: Reconfigurable die production run process variance

As the table shows, the estimated process variance ($\hat{\sigma}^2$) is found to be 0.97 mils^2. This is an order of magnitude greater then the process variance calculated for the fixed die production run of the same target shape (recall that the fixed die variance was found to be 0.098 mils^2). The increase in variance is expected. There is inherent variation in the die setup process due to the reconfiguration of the die between each forming cycle. This additional variation in the die is transmitted to the formed part shape.

4.8 Summary

In this chapter we presented methods for evaluating the part quality. The evaluation procedure requires measurement and registration of the formed part. The part quality was described in terms of maximum, RMS and mean error. The process performance was described in terms of the process mean shift and variance. Possible system noises/disturbances were be presented and quantified where practical. The performance of a stretch forming process utilizing a fixed die was compared to the same process utilizing a reconfigurable die. It was shown that the reconfigurable die resulted in an equivalent mean shift and an increase in the process variance as compared to the fixed die.

CHAPTER

5

EXPERIMENTS AND ANALYSIS OF DATA

This chapter will evaluate the performance of the reconfigurable die stretch forming process under Cycle to Cycle control. As before, the part quality will be analyzed according to the procedures detailed in chapter 4. Mean shifts and variances will be calculated and compared to the open loop processes also discussed in chapter 4. The process yield will be compared using the Expected Quality Loss Function.

5.1 Reconfigurable Die Performance Under CtC Control

The reconfigurability of the discrete die allows for cost savings from die manufacture, setup, and storage. However, the overall performance of the reconfigurable die, as implemented previously, was worse then that of the fixed die. The process was further off-center and had more variance. These two traits would signify the need for some form of feedback control to improve part quality. Implementing feedback control over the stretch forming process is difficult at best. Feedback control requires knowledge of the target shape, die shape, and part shape, as well as the ability to adjust the shapes as required. Figure 38 details a simplified control loop for the stretch forming process.

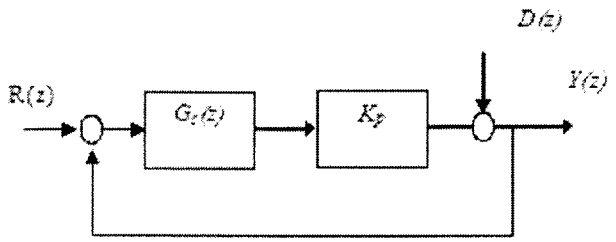

Figure 38: Basic block diagram for closed loop shape control.

G_c is the controller gain, determined by the user, K_p is the plant or process gain, which represents the process model. R(z) is the reference input, Y(z) is the output, and D(z) is the disturbance. Diagram from Pi [10]

The target, or reference, shape is a geometrical representation of the desired part and can be changed at any time. It should be identical for both monolithic and discrete die forming processes. The die shape is dependent on the target shape. Therefore, changing the target shape should effect changes in the die shape(s).

The monolithic and discrete die shapes are adequately known. Adjusting, or reshaping, these dies is more complex. The shape of a monolithic die is only adjustable through rework. Generally, rework on a monolithic die is only performed during the trial-and-error period described earlier, for incidental damage, or for routine maintenance. It is a time, money, and labor intensive process and rarely cost effective to do on a part-by-part basis. In contrast, the discrete die can be reshaped very simply with little down time and minimal labor. On the laboratory-scale stretch forming press, the reshaping process is essentially a total reforming of the die shape. More sophisticated discrete dies could be reconfigured on a pin-by-pin basis.

Measurement of the formed part shape is the most complex workpiece of information required. The methods for collecting and acting on this information do not depend on the die type (monolithic or discrete). Unfortunately, it is not practical to take measurements of the part shape in-process (i.e. while the part is being formed). It is exceedingly difficult to take accurate in-process measurements of the part shape with current methods and technology. In addition, stresses transmitted to the part from the die and material stretching apparatus (clamps) during forming cause springback to occur in

the part when the load is removed. This springback deforms the part shape beyond an amount that can be consistently predicted within the required accuracy. The forming process must be run to completion before any part measurements can be taken. This is true for both die types.

The reconfigurable die lends itself well to implementation of feedback control due to the ease of die reshaping. Unfortunately, uncertainties associated with part measurement and the process model, and the inability to change the die shape while the part is under load, hinders us from implementing this feedback control in-process. Cycle-to-Cycle (CtC) feedback control is a viable alternative.

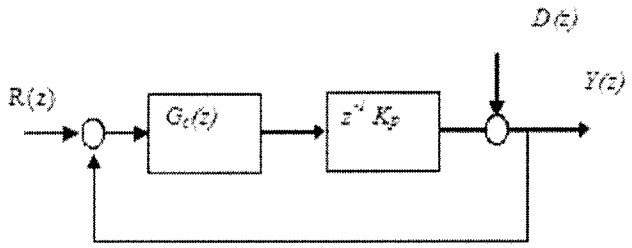

Figure 39: Basic block diagram for CtC shape control.

The plant gain Kp has a one cycle delay. Diagram from Hardt [3]

As mentioned previously, the overall performance of the fixed and reconfigurable forming processes is defined by the magnitudes of the resulting mean shifts and variances. The mean shifts and variances are dependant on the states and properties of the material and machinery.

Both die types produced unacceptable mean shifts when run under open loop control. Closed loop, or feedback, control would allow us to re-center the process once a mean shift is detected by reshaping the die.

5.1.1 CtC Parameters

The process parameters will remain identical to those of the reconfigurable die production runs. The only change will be the implementation of CtC closed loop control in place of the open loop control used previously. We will use the SCA controller described in Section 3.3 to control this production run (the matrix form of the controller is detailed in Figure 40).

$$\underset{(MN,1)}{\begin{bmatrix} {}_1d_i \\ {}_2d_i \\ \vdots \\ {}_{MN}d_i \end{bmatrix}} = \underset{(MN,1)}{\begin{bmatrix} {}_1d_{i-1} \\ {}_2d_{i-1} \\ \vdots \\ {}_{MN}d_{i-1} \end{bmatrix}} + \underset{(MN,MN)}{\begin{bmatrix} {}_1g_C & 0 & 0 & 0 \\ 0 & {}_2g_C & 0 & 0 \\ 0 & 0 & \ddots & 0 \\ 0 & 0 & 0 & {}_{MN}g_C \end{bmatrix}} x \left(\underset{(MN,1)}{\begin{bmatrix} {}_1p_{ref} \\ {}_2p_{ref} \\ \vdots \\ {}_{MN}p_{ref} \end{bmatrix}} - \underset{(MN,1)}{\begin{bmatrix} {}_1p_{i-1} \\ {}_2p_{i-1} \\ \vdots \\ {}_{MN}p_{i-1} \end{bmatrix}} \right)$$

Figure 40: SCA controller in matrix form.

5.1.2 CtC Process results

Eleven parts were formed using the parameters detailed in Table 2. Parts 1 and 2 are used by the SCA controller in the system identification procedure. The die shapes used to form these parts are intentionally off-target in order to increase the accuracy of the process model. Part 3 is considered the first "controlled" part. The Maximum, RMS, and Mean errors were calculated for each part using the equations detailed previously. The results are plotted in Figure 41.

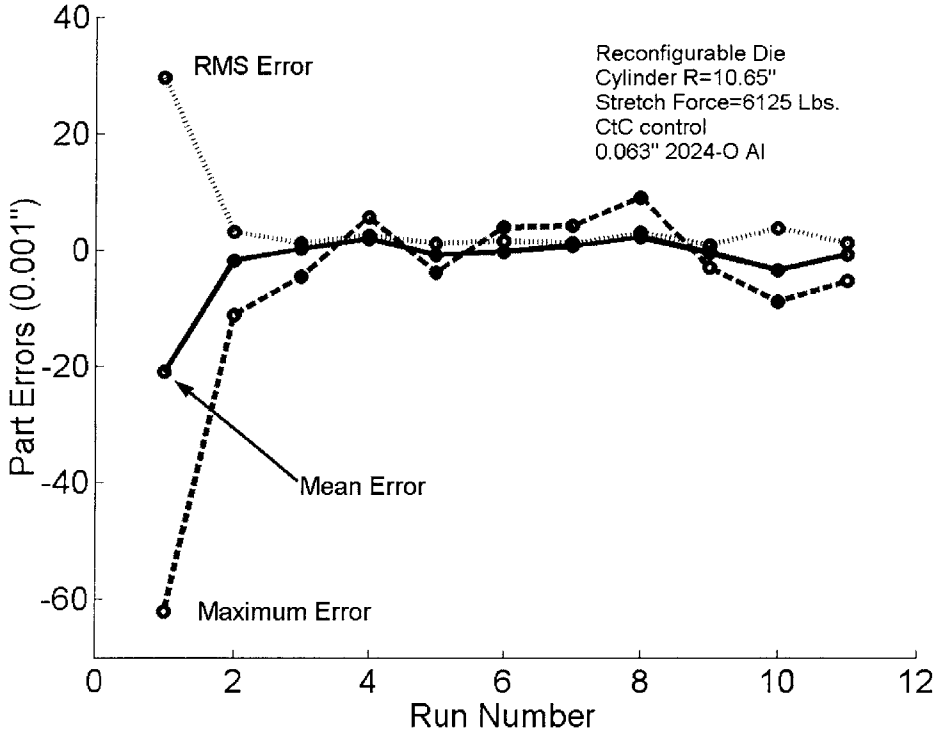

Figure 41: CtC production run errors

5.1.3 CtC Process Centering

The mean error of the process is evaluated using the procedures detailed previously. The data shows that the steady state mean error of the process is centered about 0.047 mils. This is shown in greater detail in Figure 42.

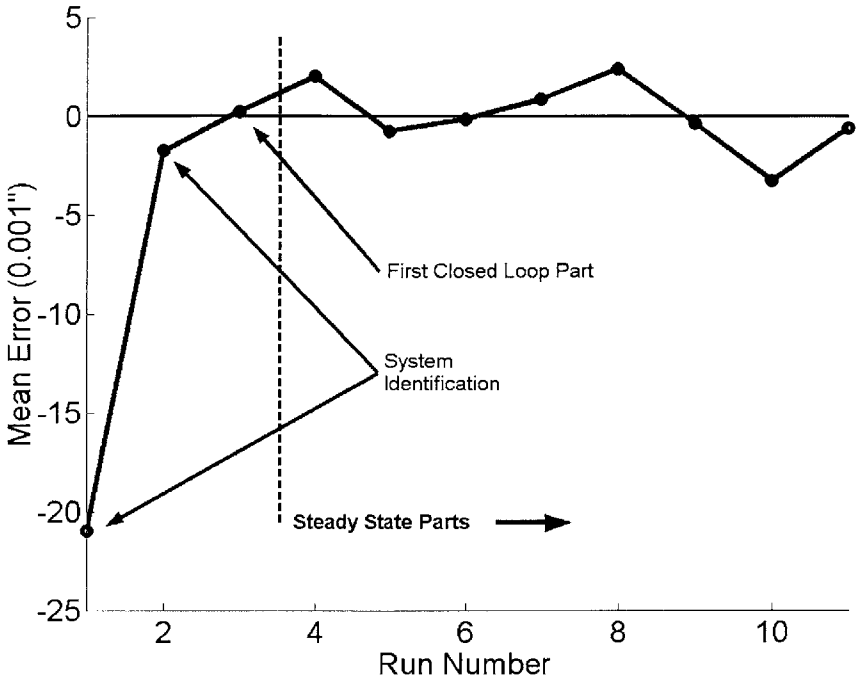

Figure 42: CtC production run mean error

As is clearly seen in Figure 42, implementation of CtC feedback control into the forming process successfully re-centered the process mean. As mentioned previously, Parts 1 and 2 are used to form the system identification. This information was used to predict a model of the system. The model was fed back to the SCA controller which adjusted the die accordingly to form the first closed loop part (Part 3). The resulting error of this part was also analyzed. The model was further refined and then used to form the Part 4. We consider the process to be in steady state after the first closed loop part (Part 3). The steady state mean error of the process is calculated using the mean error of Parts 4-11. Parts 1-3 are considered transient since these parts are used to define the process model.

5.1.4 CtC Process Variance

The steady state process variance of this production run is again calculated using Equation 21 and detailed in Table 5. Parts 4-11 are considered steady state.

S	1.78 mils
n	8
C_4	0.965
$\hat{\sigma}^2$	3.38 mils^2

Table 5: CtC production run process variance

As the table shows, the estimated process variance ($\hat{\sigma}^2$) is found to be 3.38 mils^2. This is an order of magnitude greater then the process variance calculated for the open loop (OL) reconfigurable die production run of the same target shape (recall that OL reconfigurable die variance was found to be 0.97 mils^2). This further increase in variance is expected due to the effects of CtC variance amplification predicted in Section 3.1.3. This additional variation in the die is transmitted to the formed part shape.

5.2 Evaluation of Control Methods

For most sheet metal forming processes it is desirable to minimize both the error and the variation in the formed parts. This results in better consistency and improved assembly quality. This is especially true when dealing with complex assemblies such as airframes, car bodies, etc... We have examined several sheet metal forming methods in the previous sections. We have also observed the resulting differences in part quality. These are summarized in Table 6.

Forming Method	**Mean Shift (mils)**	**Variance (mils^2)**
Fixed Die	-4.69	0.098
Reconfigurable Die	-4.79	0.97
Reconfigurable Die w/ CtC Control	0.047	3.38

Table 6: Forming method performance summary

We have observed that the implementation of a reconfigurable die with CtC control has improved the process centering by two orders of magnitude. Unfortunately, this has also resulted in an increase in the process variance by over one order of magnitude. This can be observed graphically in Figure 43.

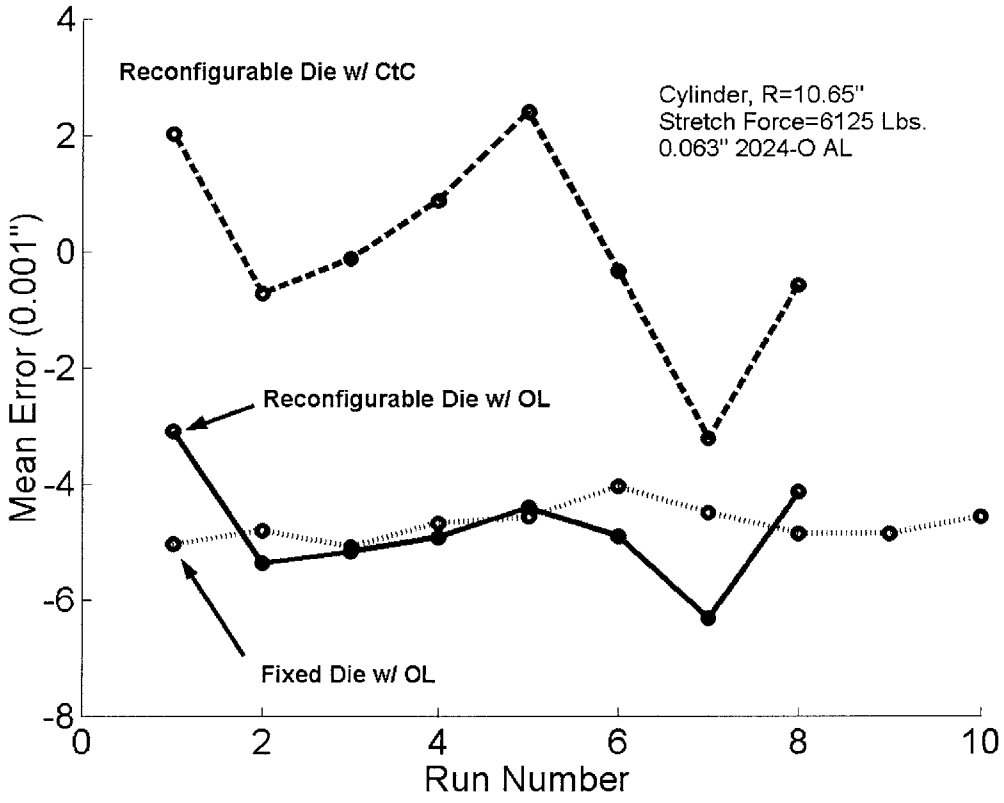

Figure 43: Process mean error for various forming methods

It can be observed that application of CtC control reduced the mean error but caused an increase in the process variance.

It is useful to determine which forming method produces the greatest part yield. We can utilize the Expected Quality Loss Function (EQL) to analyze this [20].

$$E\{L(x)\} = k\sigma^2 + k(\mu - x^*)^2$$

Equation 23

Where:

$E\{L(x)\}$ = *Expected quality loss*

k = *Cost penalty associated with deviation*

σ^2 = *Process variance*

$\mu - x^*$ = *Mean shift (μ=process mean, x^*=target mean=0)*

Equation 23 quantifies the costs associated with variance and mean shift. We will assume that k is equal to unity for the purposes of our comparison. The actual weight of this factor would depend on the specific application. Table 7 lists the expected quality loss using the values in Table 6.

Forming Method	***E{L(x)} (mils^2)***
Fixed Die	22.09
Reconfigurable Die	23.91
Reconfigurable Die w/ CtC Control	3.38

Table 7: Expected Quality Loss for forming methods

Table 7 clearly shows that a stretch forming operation utilizing a reconfigurable die under CtC control is superior to the reconfigurable die under open loop control. Reverse calculation shows that the mean shift of the reconfigurable die production run would have to be reduced to within ±1.55 mils (or 32% of the present mean shift) before the process yields would be similar.

5.3 Summary

The reconfigurable die is intended to serve manufacturers as a means to reduce cost of goods sold. This can be achieved in several ways. The first is to reduce tooling and setup costs as was discussed previously. The second is to improve the yield (or efficiency) of the production process. This results in less waste and more acceptable parts. Remember, the business of a business is to make money. This explains why most manufacturers are not necessarily driven to produce the *best* parts but to produce parts that are *good enough*. This is because "good enough" parts will satisfy the part criteria, and can therefore be sold, just as well as the "best" parts.

This chapter weighed the pros and cons of applying CtC control to the reconfigurable die stretch forming process. The mean shift and variance for the CtC reconfigurable die process was compared to that of the OL fixed die and OL reconfigurable die processes. The Expected Quality Loss Function was used to evaluate the process yields. It was shown that the reconfigurable die under CtC control produced the highest yield of acceptable parts.

CHAPTER

6

CONCLUSIONS AND GUIDELINES FOR FUTURE WORK

This thesis sought to validate the use of Cycle to Cycle control in a multiple input-multiple output process. Specifically, this control method was applied to sheet metal stretch forming using a reconfigurable die. The mechanics of stretch forming and current industrial applications were discussed. Several possible control methods were presented as well as a methodology to evaluate their performance. These control methods were implemented during several production runs. The experiments performed showed that a reconfigurable die under CtC control performed better than the status quo monolithic die under open loop control. This information should encourage manufacturers to transition to this technology.

The target part in these experiments was a simple cylindrical shape. Although a cylinder is a common shape, most manufacturers will wish to produce more complex shapes as well. Toroids, spheres, and saddles are slightly more complex. CtC experiments performed for toroids and saddles of slight curvature are presented in Appendix A. It would be useful to know how the process responds to these shapes when the target part has greater curvature. It would also be interesting to see how the system responds to asymmetrical and non-uniform parts.

SCA generates the process model during the first two forming cycles. The model is largely dependent upon the target shape since the SCA does not account for coupling. These first two formed parts are usually wasted since the error is often too great. It would be useful to know the robustness of the process model. For example, suppose the manufacturer wishes to make a run of cylindrical shapes followed by a run of toroidal

shapes. Experiments in which a slight target shape change was introduced midway through a run were performed. It was observed that the process stayed within acceptable tolerance levels despite the change in target shape (these results are presented in Appendix A). It would be interesting to observe how the process responds to more severe changes in target shape.

Rzepniewski [19] has proposed the CSC algorithm (discussed in section 3.4) as a more accurate process model of sheet forming with a reconfigurable die. Simulated results seem to concur. This model should be experimentally compared to the DTF and SCA algorithms to verify the simulations.

The system identification procedure requires two forming cycles that often result in unacceptable parts. This represents a considerable waste of time and money. It would be useful to reduce the number of system identification cycles. The obvious solution is to improve the process model. It might also be possible to build a "shape library". This could be a database of process gains for particular shapes. Manufacturers could draw upon this database to "tune" their initial die guesses.

REFERENCES

1 Parris, Andrew, "Precision Stretch Forming for Precision Assembly", *Ph.D. Thesis, Department of Mechanical Engineering, MIT*, June 1996.

2 Valentin, V. M., "In-Process Strain Control of Stretched Formed Sheet Metal Parts", *S.M. Thesis, Department of Mechanical Engineering, MIT*, June 1999.

3 Hardt, D.E., Boyce, M. C., Osterhout, K. B., Karafilis, A., "A Flexible Forming System for Sheet Metal", *18th Annual NSF Conference on Design and Manufacturing Systems Research*, Atlanta, GA, Jan. 1992

4 Burrous, D.W., Technology Specialist, Northrop Grumman Co., Commercial Aircraft Division, Dallas, TX., Personal correspondence to M. Valjavec, July 1998.

5 Robinson, R. E., "Design of an Automated Variable Configuration Die and Press for Sheet Metal Forming", *S.M. Thesis, Department of Mechanical Engineering, MIT*, February 1987.

6 Valjavec, M., "A Closed-Loop Shape Control Methodology for Flexible Stretch Forming Over a Reconfigurable Tool", *Ph.D. Thesis, Department of Mechanical Engineering, MIT*, February 1999.

7 Papazian, J. M., Hoitsma, D., Kutt, L., Melnichuk, J., Nardiello, J., Pifko, A., Schwarz, R. C., "Reconfigurable Tooling for Sheet Metal Forming", *Sheet Metal Forming Technology* edited by Demeri, M. Y., The Minerals, Metals & Materials Society, Warrendale, PA, 1999.

8 Norfleet, W. A., "Algorithms for Closed Loop Shape Control", *S.M. Thesis, Department of Mechanical Engineering, MIT*, June 2001.

9 Papazian, "Tooling For Rapid Sheet Metal Parts Production", *6Th Joint Faa/DoD/NASA Conference on Aging Aircraft*, San Francisco, CA., Sept 2002.

10 Pi, A., "Effects of Uncertainty on Closed Loop Shape Control in Stretch Forming", *S.M. Thesis, Department of Mechanical Engineering, MIT*, Sept. 2002.

11 Taguchi, G., "Introduction to Quality Engineering." *Asian Productivity Organization*, UNIPUB, White Plains, NY, 1986.

12 Montgomery, D.C., "Introduction to Statistical Quality Control." *John Wiley & Sons, Inc.*, 2001.

13 Webb, R. D., "Adaptive Control of a Flexible Die System for Forming Sheet Metal Parts", *S.M. Thesis, Department of Mechanical Engineering, MIT*, June 1981.

14 Webb, R. D., "Spatial Frequency Based Closed-Loop Control in Sheet Metal Forming", *Ph.D Thesis, Department of Mechanical Engineering, MIT*, May 1987.

15 Ousterhout, K.B., "Real-Time Control of a 3D Sheet Forming Process", *Ph.D. Thesis, Department of Mechanical Engineering, MIT*, Sept. 1991.

16 Rzepniewski, A.K., Hardt, D.E., "Multiple Input-Multiple Output Cycle-to-Cycle Control for Manufacturing Processes." *Second Annual Singapore MIT Alliance Symposium*, Singapore, Jan. 2003.

17 Siu, G. T.-S., "Cycle-to-cycle Feedback Control of Manufacturing Processes," *S.M. Thesis, Department of Mechanical Engineering, MIT*, Feb. 2001.

18 Rzepniewski, A.K., Hardt, D.E., Vaughan, C.D., "Cycle-to-Cycle Control of Large, Coupled-Effect Multivariable Manufacturing Processes with Process Model Uncertainty", *2004 ASME International Mechanical Engineering Congress*, Anaheim, CA. Jan. 2003.

19 Rzepniewski, A.K., Hardt, D.E., "Gaussian Distribution Approximation for Localized Effects of Input Parameters." *Second Annual SMA Symposium*, Singapore, Jan. 2003.

20 Hardt, D. E. "Expected Quality Loss", Manufacturing Process Control Class Notes, Department of Mechanical Engineering, MIT, March, 2003.

APPENDIX A

An experiment was performed to test the disturbance response of the SCA control method. We began with the eleven part CtC production run presented in section 5.1. The process was disturbed by substituting the cylindrical target shape used to form the first eleven parts for a toroidal target shape. Five more parts were formed according the process parameters in Table 8.

Parameter	Value
Pin size	0.5 inch
Stretch Force	6125 lbs.
Part Material	Al 2024-O, 19.5 x 5.5 x 0.063 inches
Final part footprint	4.5 x 5.0 inches
Force trajectory	Pre-stretch, wrap, no post stretch
Control mode	Force control
Interpolator	Elvax 360 (0.535 in. thick) covered with two layers of Teflon
Target Shape	10.65" radius reference cylinder
Disturbance Shape	Toroid, Ry=10.65", Rx=45"

Table 8: Machine parameters used to form toroid disturbance production run

Note that the only process parameter changed was the target shape. The production run errors are presented in Figure 44.

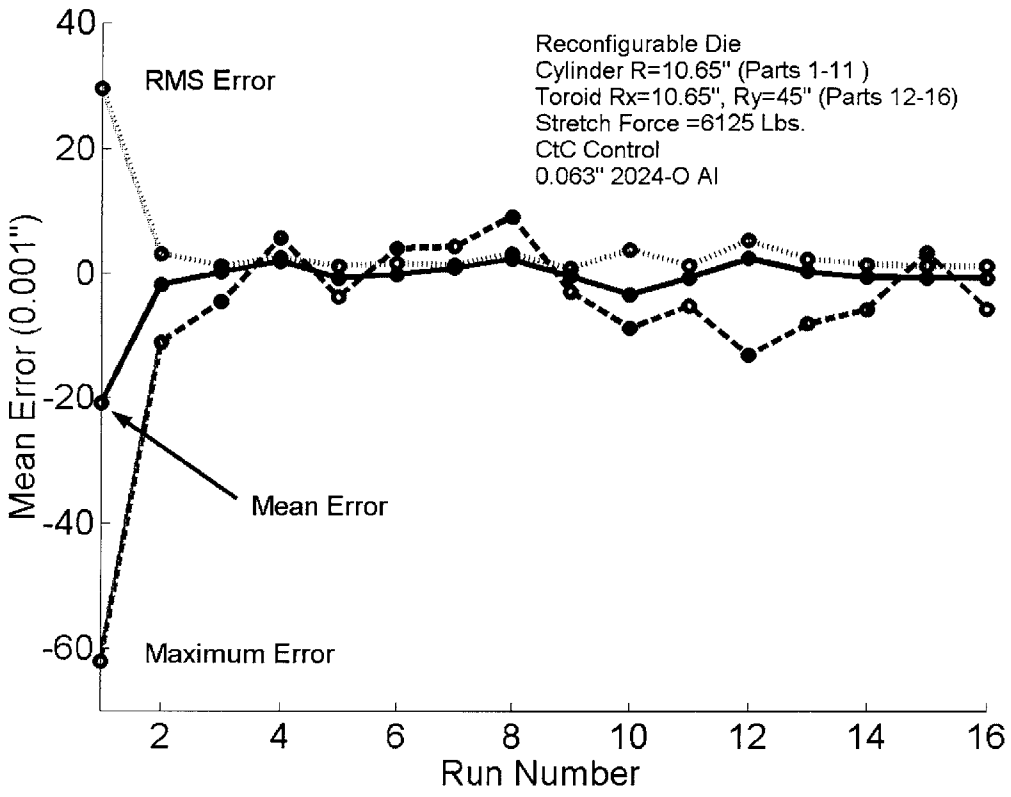

Figure 44: CtC production run mean error with toroid shape disturbance

A toroid shape disturbance is injected at part 12

The effects of the disturbance can be observed at part 12. We can see the CtC controller adjusting the process inputs to re-center the process mean. Unfortunately, the resulting disturbance was not much greater then the variation present in the process. This is most likely due to the minimal target shape change. The disturbance response would be easily visible if a more drastic shape change were introduced.

APPENDIX B

Several past researchers have applied the algorithms discussed in section 3.2 with varying results. These are presented in this appendix for comparison.

Webb applied Algorithm #1 to a matched-die sheet forming process. Results from a five part production run are presented in Figure 45.

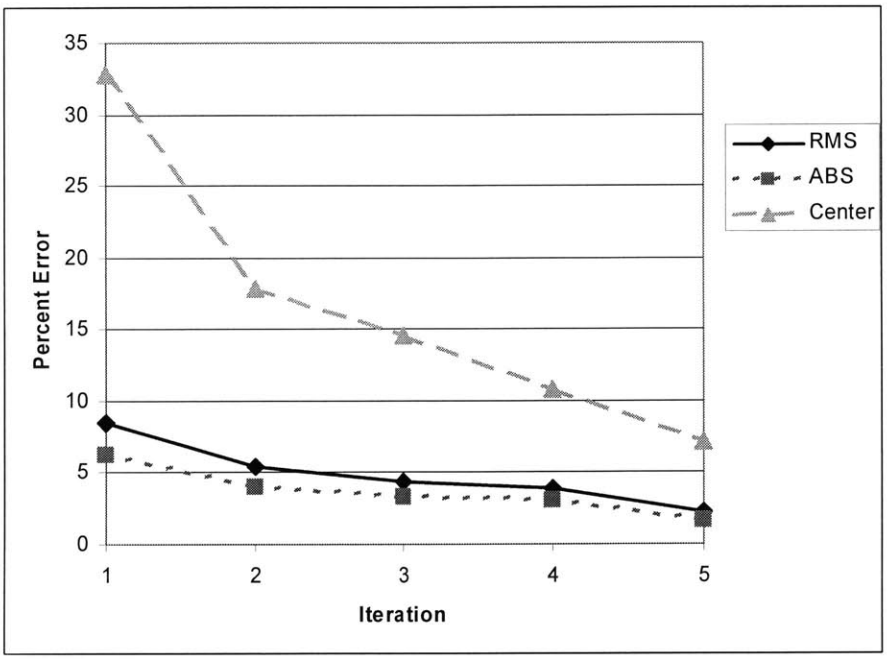

Figure 45: Algorithm #1 results from Webb [14]

This algorithm was applied to the matched-die sheet forming process.

As observed in Figure 45, Algorithm #1 gradually reduces the part shape error. The lack of a system identification step is most likely the cause of the slow convergence.

Valjavec applied Algorithm #2 (DTF) to the stretch forming process. Several forms of this algorithm were developed to speed the convergence. The results from a four part production run of one of these forms, the Backward Difference method, are presented in Figure 46.

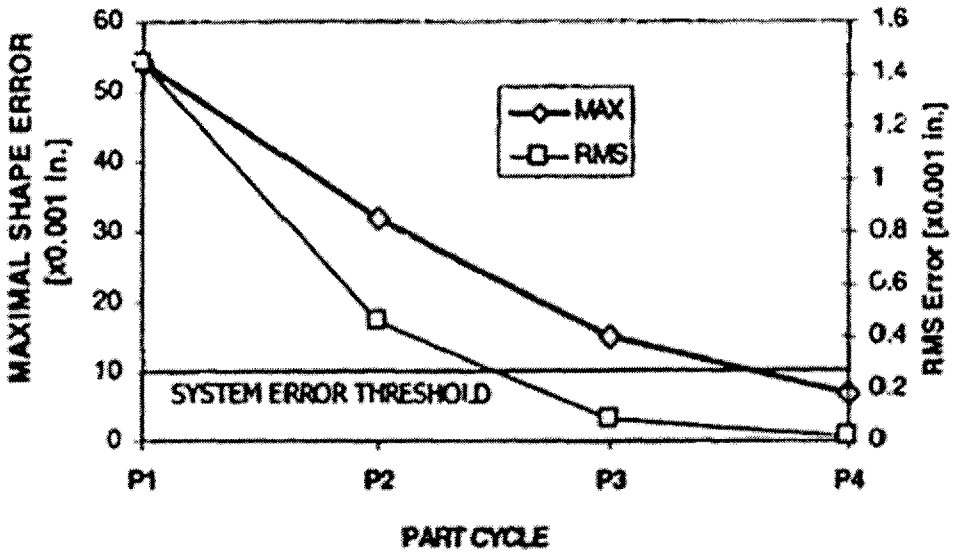

Figure 46: Algorithm #2 results from Valjavec [6]

This algorithm was applied to the stretch forming process.

The SCA experiments performed in this research were run on the same machinery that Valjavec used for his experiments. One of Valjavec's experiments was duplicated to assess the status of the stretch forming machinery. The process parameters were identical to those used in Valjavec's experiment as well as the SCA experiments performed in chapter 5 (refer to Table 2). The results are presented in Figure 47.

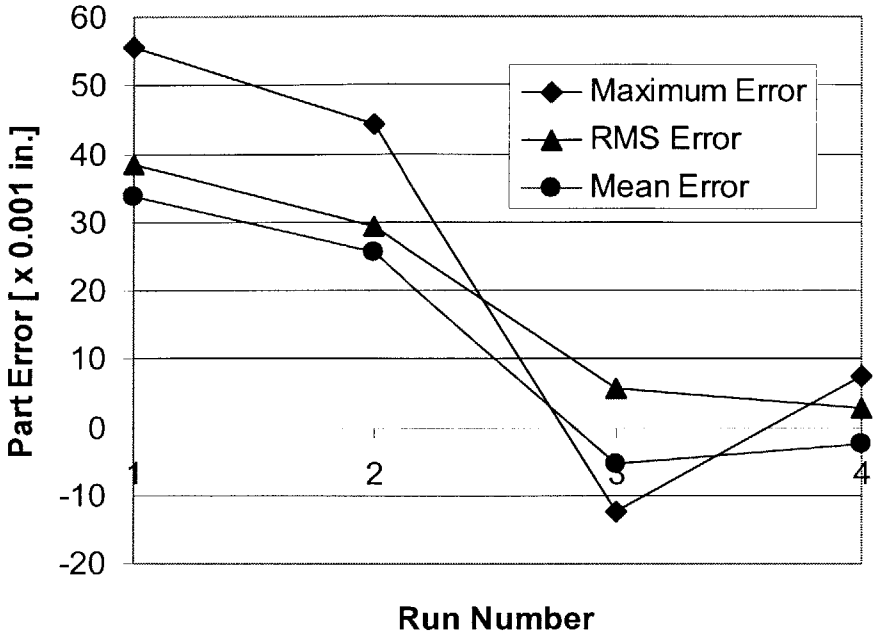

Figure 47: Algorithm #2 (DTF) results from this author.

This algorithm was applied to the stretch forming process. The process parameters and controller were identical to Valjavec's DTF experiment shown in Figure 46.

It can be observed that the results in Figure 46 and Figure 47 are similar. This benchmarks the mechanical status of the stretch press and allows us to compare the performance of Algorithm #1 to Algorithm #2 and others.